CONTROLLING SIBLING PROTEIN ORIENTATION AND CONFORMATION VIA NATIVE BINDING INTERACTIONS

By

Kevin M. Zurick

Dr. Matthew T. Bernards, Dissertation Supervisor

December 2013

The undersigned, appointed by the dean of the Graduate School, have examined the [thesis or dissertation] entitled

CONTROLLING SIBLING PROTEIN ORIENTATION AND CONFORMATION VIA NATIVE BINDING INTERACTIONS

presented by Kevin Zurick,

a candidate for the degree of doctor of philosophy,

and hereby certify that, in their opinion, it is worthy of acceptance.

_____

Professor Matthew Bernards

_____

Professor Patrick Pinhero

_____

Professor Paul Chan

_____

Professor Qingsong Yu

DEDICATION

  This dissertation is dedicated to my parents, Karen and Barry Zurick, and my grandparents, Alice and Vern Lauher, for their continuous love, support, and encouragement throughout my life. Without your love and support I never would have been able to complete my undergraduate or graduate degrees.

ACKNOWLEDGEMENTS

My deepest thanks to my dissertation supervisor, Dr. Matthew Bernards, for the opportunity to work in his group and pursue biomaterials research. His honesty and professionalism is top notch, and I will use the skills he taught me as a researcher for many years to come. It was truly special to work with Dr. Bernards, and I wish him the best of luck in all future endeavors.

I would also like to extend thanks to the rest of my dissertation committee: Dr. Patrick Pinhero, Dr. Paul Chan, and Dr. Qingsong Yu. Many thanks for their time, criticisms, and evaluation of my work. It was an honor to have you all on my committee.

Finally, I would like to thank Robert Holtsmith for his generous donation to the College of Engineering. Without his fellowship, I would not have been able to attend MU and complete my doctoral studies.

TABLE OF CONTENTS

LIST OF ILLUSTRATIONS

CHAPTER 1. INTRODUCTION

1.1.   Background

Bone grafting is a surgical procedure in which missing bone is replaced in order

to repair fractures they may not otherwise heal naturally. Typically, bone fractures will

heal completely if they are small, but critical size defects cannot heal without some sort

of scaffold to provide support for cell regrowth. Traditionally, bone is taken from

another area on the patient (autograft), taken from a cadaver (allograft) or taken from

an animal source (xenograft) and implanted in the defect site. However, these

approaches do not always work for all types of injuries. Autografts cannot be performed

if the site is very large and also pose an additional risk to the patient in the form of

infection at the donor site. Likewise, allografts and xenografts run the risk of rejection

and are not always readily available. Because of this, other methods have been devised

to address the needs of bone graft patients, including synthetic bone scaffolds.

An ideal synthetic bone scaffold needs to meet a number of characteristics,

including biocompatibility, adequate mechanical properties, osseoconductivity,

adequate pore size/pore interconnectivity, and the ability to be resorbable in the *in vivo*

environment.[1-3] Due to the wide range of requirements, no single component system

can meet all of the requirements for an ideal bone tissue scaffold. Because of this, many

groups have focused on creating a multi-component system similar to that of real bone.

Most of these systems pair a polymer with some form of calcium phosphate in an

attempt to mimic the collagen-hydroxyapatite composite which comprises a majority of native bone tissue.[4,5] While many of these newer, multi-component systems can meet one or more of these requirements, there is still no composite bone scaffold which can meet all of these characteristics. With that in mind, it is useful to examine the structure and composition of bone to gain insight into how these composite scaffolds may be improved.

1.2   Collagen

Collagen type I is the most abundant protein in the body and bone tissue and comprises 10 – 30 % of mineralized bone tissue. Demineralized bone tissue contains 90 – 97 % collagen.[6,7] It is formed by enzymatic polymerization between amino and carboxyl groups of amino acids. The general amino acid sequence is (-Gly-X-Y-)$_n$, where X is any other amino acid (typically proline) and Y is any other amino acid (usually hydroxyproline).[8] Type I collagen consists of three left-handed polypeptide chains, which intertwine to from a right-handed helix. Two of the three peptide chains are identical, while the third differs only slightly in composition. The two identical chains are referred to as α_1 chains, while the third chain is referred to as the α_2 chain.[9] Over 95% of the collagen molecule follows the Gly-X-Y motif.[6,7] The presence of glycine at every third amino acid allows the chains to pack tightly together into a triple helix, which is stabilized by hydrogen bonding between the chains. The remaining 5% of the molecule does not follow this motif and is not triple-helical. The nonhelical portions are located at both ends of the molecule and are referred to as telopeptides, and are also the sites where cross-linking with other collagen molecules can occur.[6,7]

However, collagen does not occur as isolated molecules in the body. Rather, the collagen molecules aggregate together to form fibrils which are usually about 300 nm in diameter and are easily seen with electron microscopy.[7,8] The fibrils then come together to former larger collagen fibers.[10] The fibrils are staggered throughout the fiber by 64-67 nm, resulting in what is known as *D*-periodicity, with *D* being the fundamental repeat distance between fibrils. This periodicity is heavily influenced by both pH and ionic content of the solution in which it occurs.[11-13] *D*-periodicity results in fibril overlap regions that are about 25 nm in length and gap regions between fibrils which are about 40 nm in length. It is thought that protein binding, ion and protein transfer/diffusion, and mineralization of the collagen fibrils occurs in these gap regions.[6,14]

1.3   Hydroxyapatite

Hydroxyapatite (HA or HAP) is the primary mineral constituent of bone, and comprises 70-90 % of mineralized tissue, with the remainder consisting of proteinaceous material. Alone, hydroxyapatite is somewhat brittle but when formed in a collagen matrix it adds rigidity and strength to the collagen matrix.[6,15,16] Pure hydroxyapatite has the formula $Ca_{10}(PO_4)_6(OH)_2$, but the OH group can be substituted with other ions, including fluoride, carbonate, chloride, magnesium, strontium, and others, which are typically the impurities found in biological hydroxyapatite.[6] Bone mineral is also typically less crystalline than pure hydroxyapatite, with a size between 10 – 40 nm in the longest direction and is almost always less than 2 nm thick with a plate-like shape.[17,18] The mechanism by which HA minerals form on collagen fibrils is poorly

understood, it has been suggested that the mineralization process is aided by noncollagenous proteins, specifically SIBLING proteins.[19-23]

1.4 SIBLINGs

1.4.1 General Characteristics

The protein component of bone has been shown to be ~90% collagenous, while the remaining 10% of the protein content is believed to play a role in bone formation, growth, repair, and cellular adhesion to the matrix.[6,23] The primary group of non-collagenous proteins found in bone are the SIBLING (small integrin-binding ligand, *N*-linked glycoprotein) family of proteins and they are believed to play a key role in these processes.[23] The SIBLING family of proteins consists of five members: osteopontin (OPN), matrix extracellular phosphoglycoprotein (MEPE), bone sialoprotein (BSP), dentin matrix protein 1 (DMP1), and dentin sialophosphoprotein (DSPP). The SIBLING proteins have a number of shared characteristics including a collagen binding domain, a HA binding domain, and a cell binding arganine-glycine-aspartic acid (RGD) sequence. Additionally, they are all located on the same human chromosome (4q21).[23] All of the proteins are acidic and contain a high degree of random coil structure. Furthermore, all of the proteins are post-translationally phosphorylated and have been immunolocalized in mineralized tissues.[23-26] Together, these characteristics suggest that the SIBLING family of proteins play an important role in bone development by facilitating collagen fibrillogenesis, cellular adhesion, mineral nucleation, and mineral maturation. Because this work is focused on the early stages of bone formation, MEPE is not being considered due to the fact that it is not expressed by bone cells until the early stages of

bone formation are complete and because it has been shown to be a potent inhibitor of mineralization both *in vitro* and *in vivo* and therefore is not expected to play a role in the induction of early biomineralization, cell binding, or fibrillogenesis.[23] Likewise, DMP1 is not being investigated due to its perceived role in mineral maturation, which suggests that it is primarily involved in the later stages of bone growth.[23] DMP1 is believed to regulate the mineralization process, possibly mediating the transformation of amorphous calcium phosphate to crystalline HA.[23] Furthermore, neither MEPE nor DMP1 have been found ahead of the mineralized front of bone, suggesting that they are not present for the earliest stages of bone formation.[23] Because this work is focused on the native binding interactions that occur in the earliest stages of bone tissue synthesis, only BSP, DPP, and OPN will be examined in detail in this work.

1.4.2 Bone Sialoprotein

BSP was initially isolated from bone and is comprised of 281-327 amino acids with a molecular weight of 60-80 kDa.[24] Similar to OPN, BSP has strong Ca^{2+} chelating properties due to an overall negative charge and a high degree of phosphorylation.[24] Additionally, it has been shown that the collagen-BSP interaction promotes HA formation in several *in vitro* systems.[27,28] BSP exhibits a binding preference for triple-helical collagen, and when bound to collagen it promotes HA nucleation *in vitro*.[27] BSP has also been shown to enhance both osteoblast differentiation and matrix mineralization *in vitro* in osteoblasts genetically engineered to overexpress BSP.[28] In another study, no statistically significant difference in MC3T3-E1 cell binding was found when comparing BSP specifically bound to collagen versus BSP randomly adsorbed to

tissue culture polystyrene, suggesting that BSP may have conformational flexibility around its RGD group.[29]

1.4.3 Dentin sialophosphoprotein

DSPP was originally thought to only occur in dentin, but has since been found in bone tissue.[23,30] DSPP is cleaved into two fragments in bone and dentin, dentin phosphoprotein (DPP) and dentin sialoprotein (DSP).[31] . DPP was chosen for this work over DSS because DPP contains the RGD sequence, the collagen-binding domain, and the HA-binding domains of the DSPP molecule. DPP is a highly negatively charged molecule comprised of 751 amino acids in humans with a molecular weight of 100-140 kDa.[23,26] It also has a high degree of phosphorylation.[21,26,31] It is the major non-collagenous protein of the dentin extracellular matrix (ECM) and becomes soluble only after the ECM has been demineralized.[31] Additionally, it contains a highly repeated DSS (aspartic acid-serine-serine) group which is believed to aid in Ca^{2+} binding and subsequent HA mineralization. In one representative mineralization study, Milan *et al*. showed that DPP significantly promotes the rate of HA crystal growth when specifically bound to collagen I.[20] The DPP subdomain also contains an arganine-glycine-aspartic acid (RGD) cell binding motif, which encourages cell binding by interacting with transmembrane integrins on cells. DPP has also shown a strong affinity for collagen binding.[6,22,24-26,30]. Because DPP contains both an RGD cell binding moiety and it has been localized ahead of the mineralized front of bone and dentin, it is also possible that it plays a role in mediating cell binding in these developing tissues

1.4.4 Osteopontin

OPN was originally isolated from bone tissue and is comprised of 260-317 amino acids with a molecular weight of 45-75 kDa.[25] It exhibits Ca^{2+} chelating properties which are due to a high amount of phosphorylation and negative charge.[22,25] Depending on the degree of phosphorylation and concentration present, OPN has been shown to inhibit or encourage HA nucleation in an *in vitro* gelatin-gel system.[32] Since its initial discovery, OPN has since been found in other tissues beyond bone where calcium phosphate mineralization occurs.[22,23,25] OPN has been shown to promote osteoblast-like cell binding, and its cell binding capabilities are enhanced when specifically bound to hydroxyapatite and collagen.[29,33,34] Finally, OPN also has the highest collagen binding affinity of any of the SIBLINGs, at 5 µM.[23]

1.5 Immune Response to Biomaterials

Immediately upon implantation in the body, a biomaterial is covered by proteins present in blood, and later by cells associated with the healing process that fill the wound site. These adsorbed biomolecules and cells influence the subsequent physiological response to the implanted material. If the immune system recognizes the material as a foreign body, it will begin to attack the biomaterial. However, the continual presence of the biomaterial prevents removal of the material and total healing of the wound site. Because of this, the immune system will continually attack the surface of the biomaterial, eventually causing the biomaterial to be encapsulated in a mass of avascular fibrous tissue which effectively isolates it from the surrounding tissues. This is prohibitive to the healing process because the biomaterial will not

integrate fully with the surrounding tissue, resulting in an increased risk of infection or rejection of the material which can lead to further complications for the patient and costly additional procedures.

However, it may be possible to circumvent, or at least minimize, this foreign body response by controlling the adhesion, conformation, and orientation in which proteins and other biomolecules adhere to the biomaterial surface in the early stages of the wound healing process. Recent efforts have focused on controlling protein orientation with charged self-assembled monolayers (SAMs). A study by Liu et al.[35] demonstrated that OPN had a preferential orientation for endothelial cell adhesion when adsorbed to a positively charged NH_2-terminated SAM as opposed to a negatively charged COOH-terminated SAM. Similar work has been performed with antibodies.[36] More recent efforts have focused on replicating specific-protein-protein or protein-substrate binding interactions to promote natural protein orientation.[27,29,33,37,38] A study by Liu et al. [35] demonstrated that OPN had a preferential orientation for endothelial cell adhesion when adsorbed to a positively charged NH_2-terminated SAM as opposed to a negatively charged COOH-terminated SAM. Similar work has been performed with antibodies [36]. More recent efforts have focused on replicating specific-protein-protein or protein-substrate binding interactions to promote natural protein orientation [27,29,33,37,38]. Previous work by Bernards and others has examined MC3T3-E1 osteoblast-like cell binding onto surfaces covered with either OPN or BSP when the proteins were either oriented through specific binding interactions with collagen or randomly adsorbed onto tissue culture polystyrene (TCPS) substrates. A statistically significant

difference was detected in the amount of cell binding on the collagen-OPN surfaces, indicating a preferential orientation and/or conformation for MC3T3-E1 cell adhesion when OPN was specifically bound to collagen [34]. No statistically significant difference in MC3T3-E1 cell binding was found when comparing BSP specifically bound to collagen versus randomly adsorbed BSP, suggesting that BSP may have more conformational flexibility around its RGD group [29].

1.6   Focus of this work

The research presented in this work is focused on examining the native binding interactions between bone constituents and SIBLING proteins, specifically BSP, DPP, and OPN, and to use those interactions to begin developing a novel bone tissue engineering scaffold. Currently, synthetic bone technologies can only replicate the soft, inner layer of bone. This dissertation focuses on the binding interactions between different bone constituents and three SIBLINGs: BSP, DPP, and OPN. The mineralization capacity of BSP, DPP, and OPN up to 24 hours is examined at time points up to 24 hours using a collagen monolayer with morphology similar to that found in developing bone as the substrate. The cell binding capacity of DPP when randomly adsorbed to tissue culture polystyrene and when specifically bound to collagen is examined and compared to prior work with BSP and OPN. Finallly, the effects of the three SIBLINGs on early collagen fibrillogenesis is testing using an *in vitro* assay. By replicating the native binding interactions between collagen, hydroxyapatite, bone cells, and SIBLINGs, it is hypothesized that a more robust bone tissue engineering scaffold can be engineered, while still retaining the biocompatibility and osteoconductive properties of a collagen-hydroxyapatite scaffold.

CHAPTER 2. MINERALIZATION INDUCTION EFFECTS OF SIBLING PROTEINS

The following chapter was first published in a similar form in the Journal of Biomedical

Materials Research, Part A and can be located using the following information:

2.1 Introduction

In this investigation, the SIBLING proteins OPN, BSP, and DPP are studied to better formalize the individual roles that these proteins play in biomineralization. MEPE is not being considered at this time due to its known inhibitory role and DMP1 is not being investigated due to its perceived role in mineral maturation. While OPN is also perceived to play a regulatory role, it has been immunolocalized in the collagen matrix ahead of developing bone and uncertainty remains regarding its mineralization induction properties. DPP has been shown to have the capacity to strongly bind calcium ions, indicating its potential for playing a role in biomineralization.[21,26] Furthermore, OPN and BSP have also been seen to be enriched at bone-implant interfacial sites.[6,15,23,39-42] This suggests that these three proteins are the most likely candidates responsible for inducing biomineralization of the collagen matrix in developing bone.

The foci of this work are to determine the adsorption characteristics of OPN, BSP, and DPP to an aligned 2D collagen type I fibril matrix that resembles developing bone and to directly compare the mineralization induction effects of OPN, BSP, and DPP when specifically bound to this matrix. Multiple investigations have characterized the adsorption or binding of these proteins to various collagen coatings.[6,24-26,31] For example, our previous work probed OPN and BSP binding to a collagen type I tropocollagen coating on tissue culture polystyrene (TCPS).[29] However, there is noticeable variation in the levels of bound or adsorbed protein depending on the structure, type, and source of the collagen substrate. During bone formation, it has been shown that cells initially lay down a matrix composed of loosely aligned collagen type I

fibrils, which are then mineralized.[6] A similar collagen assembly would therefore be the most biologically relevant for probing SIBLING induced biomineralization. Recently, Jiang and colleagues demonstrated the self-assembly of tropocollagen into loosely-aligned collagen fibrils with characteristic *D*-periodicity, similar to that found *in vivo*, using a mica substrate.[11] The interactions between the mica surface chemistry and tropocollagen molecules were found to guide the self-assembly process, leading to a good biomimetic collagen fibril platform for conducting biomineralization investigations.

The specific roles that OPN, DPP, and BSP play in mineral formation and growth have not been fully determined. This information is of interest in bone biology and it can be used to guide the development of bone tissue engineered materials. This is one of the first direct side-by-side studies of the mineralization capacities of SIBLING proteins on a substrate that mimics developing bone. The results suggest that while minerals were seen in the presence of all three SIBLING proteins, DPP was the only protein that formed distinct mineral nodules that most closely resemble those of developing bone. This suggests that DPP may be responsible for inducing biomineralization.

2.2 Experimental Procedures

2.2.1 Materials

Ultrapure water (18.2 MΩ-cm) was obtained from a Millipore Synergy UV water purifier (Billerica, MA) and it was used for all experiments. Mica discs (10 mm diameter) were purchased from Ted Pella Inc. (Redding, CA) and were freshly cleaved immediately prior to use. Phosphate buffered saline (PBS, 150 mM, pH 7.4), KCl, NaCl, NaHCO$_3$, Na$_2$CO$_3$, KCl, K$_2$HPO$_4$, MgCl$_2$ Na$_2$SO$_4$, and tris(hydroxymethyl)aminomethane (Tris-HCl)

were purchased from Thermo Fisher Scientific (Waltham, MA). KCl-Tris buffer was prepared by dissolving 50 mM Tris-HCl and 200 mM KCl in 18.2 MΩ-cm water and adjusting the pH to 7.4 with NaOH. Bovine serum albumin (BSA) with a purity of >96% was purchased from Sigma-Aldrich (Saint Louis, MO). Heat denatured BSA was prepared by heating a 1 mg/mL solution of BSA in Tris-KCl buffer at 60 ^{o}C for 30 minutes. Type I collagen from rat tail with a purity of >90% was purchased from BD Biosciences (Bedford, MA). 4-(2-hydroxyethyl)-1-piperazineethanesulfonic acid (HEPES) was purchased from Sigma Aldrich. $CaCl_2$ and NaOH were purchased from Acros Organics (Pittsburgh, PA). The PiPer phosphate assay kit was purchased from Molecular Probes (Eugene, OR) and the QuantiChrom calcium assay kit was purchased from BioAssay Systems (Hayward, CA). 50% HNO_3 was obtained from Ricca Chemical Company (Arlington, TX) and diluted to 1.0 M using ultrapure water before use. Iodogen reagent was purchased from Pierce (Rockford, IL) and ^{125}I-Na was obtained from Amersham (Arlington Heights, IL).

2.2.2 SIBLING protein isolation procedures

BSP and OPN, were extracted from the tibiae of 10-week-old rats as described in detail previously.[43,44] The total bone protein extracts were subjected to multiple gel chromatography isolation/purification steps. The purity and identity of OPN and BSP were confirmed with polyacrylamide gel electrophoresis and Western immunoblots using antibodies specific to OPN and BSP.

DPP was extracted from the incisor dentin of 10-wk-old rats by standard procedures as described in detail elsewhere.[45,46] Briefly, the total rat dentin protein

extract was subjected to gel chromatography, ion-exchange, and size-exclusion chromatography isolation/purification steps. Fractions containing DPP were combined, dialyzed, and lyophilized for use in this study. The purity of the collected DPP was confirmed by SDS-PAGE with Stains-All staining.

2.2.3 Collagen Substrate Preparation

Collagen-coated mica discs were prepared by adapting a previously established procedure.[11] Substrates were prepared by incubating freshly cleaved mica disks with 40 µL of a 0.3 mg/mL collagen solution in KCl-Tris buffer. The discs were covered with a Parafilm square immediately after applying the collagen solution and left overnight at room temperature. Following the overnight adsorption, the substrates were rinsed with ultrapure water and dried with filtered air. The presence of aligned collagen fibrils was confirmed using atomic force microscopy (AFM). AFM was performed on an Agilent 5400 (Agilent Technologies, Palo Alto, CA). Silicon cantilevers having a force constant of 0.2 N/m and a resonant frequency of 13 kHz were purchased from Budget Sensors (Bulgaria). Images were obtained in contact mode with a resolution of 1024x1024 pixels at a rate of 3.0 lines/second using a 10 µm scanner. Images were simultaneously recorded in topography and deflection modes. All images were acquired in air at room temperature. Gwyddion freeware was used to view and analyze the images.[35]

2.2.4 Radiolabeling Procedure

BSP, OPN, and DPP were individually labeled with ^{125}I using iodogen reagent and a previously established procedure.[47] Briefly, 100 µg of iodogen was suspended in 35 µL of the desired protein solution to which 750 µCi of ^{125}I-Na (100 mCi/mL) was added.

After 5 min, the mixture was transferred to a 20 cm Sephadex G25-150 column that had

been equilibrated with PBS (pH 7.4). The column was then eluted with 15 mL of PBS and

500 µL fractions were collected. The radioactivity associated with each fraction was

determined, and the highest count radiolabeled fraction for each protein was selected

and used in all subsequent protein binding experiments.

2.2.5 Protein Adsorption Isotherms

Collagen-coated mica discs were prepared as previously described, then rinsed

with 18.2 MΩ-cm water and soaked in 1 mg/mL heat-denatured BSA for 5 hours to block

nonspecific protein binding.[125]I radiolabeled OPN, BSP, or DPP were added to 1.0 mg/mL

solutions of unlabeled OPN, BSP, or DPP to obtain solutions with specific activities of

144.0, 124.2, and 116.0 counts per minute (cpm) per nanogram of protein, respectively.

The collagen substrates were removed from the BSA solution and rinsed with 18.2 MΩ-

cm water before being incubated with varying concentrations of BSP, DPP, or OPN

solutions overnight at 4 $^{\circ}$C in a humidified atmosphere. Afterwards, they were rinsed 3

times with KCl-Tris buffer to remove loosely bound proteins. The cpm radioactivity of all

of the samples was measured with a Wizard 1470 automatic gamma counter

(PerkinElmer, Waltham, MA). The amount of protein specifically adsorbed to the surface

of the substrates was calculated by relating the cpm of each sample to the sample

surface area and specific activity of each protein exposure solution. Each protein

concentration adsorption experiment was repeated three times (n=3).

2.2.6 Freundlich Adsorption Isotherms

The Freundlich equation was developed in an attempt to empirically relate the concentration of a solute on the surface of an adsorbent to the concentration of the solute in the liquid with which the adsorbent is in contact. In this work, it was applied to the results of the ^{125}I radiolabeled adsorption isotherms to gain insight into the mechanism of binding between collagen and the three SIBLINGs tested. The Freundlich equation is shown as Equation 2.1 below.

$$\qquad 2.1$$

In the above equation, y = ng of SIBLING/mm^2, c = mg of SIBLING/mL exposure solution, with K and n being empirical constants. K is related to the capacity of the surface for adsorption, while n is related to the binding intensity of the SIBLING. The equation can then be linearized to produce Equation 2.2.

$$\qquad 2.2$$

The results of the ^{125}I radiolabeled adsorption isotherms were plotted using the linearized Freundlich equation. A linear trendline was constructed using a least squares fit and the K and n parameters for each SIBLING tested were extracted.

2.2.7 Mineralization Using Simulated Body Fluid

Mineralization on the collagen-coated mica discs with adsorbed proteins was probed using the modified simulated body fluid (m-SBF) described by Oyane *et al*.[48] Briefly, the reagents listed in Table 2.1 were dissolved in the order listed into 18.2 MΩ-cm water at 37 ^{o}C to form m-SBF. Collagen-mica substrates were prepared with adsorbed proteins as described above. However, the discs were incubated with only

one exposure concentration for each SIBLING protein to eliminate the need for

normalization between different protein-collagen substrates due to differences in the

amount of adsorbed protein. Specifically, 10 µg/mL BSP, 50 µg/mL OPN, and 32.5 µg/mL

DPP were used. Heat denatured BSA (1 mg/mL) samples were also prepared as a

control. Following the protein adsorption step, the discs were then washed with 18.2

MΩ-cm water to remove non-specifically adsorbed proteins and placed into the m-SBF

for 5, 10, or 24 hours at 37 °C. Following incubation, the samples were removed and

rinsed with ultrapure water and dried with filtered air before mineral characterization.

2.2.8 Mineral Morphology Analysis

The morphology of the minerals formed in SBF was examined using AFM. AFM

was performed on an Agilent 5400 with silicon cantilevers having a force constant of 0.2

N/m and a resonant frequency of 13 kHz. Images were obtained in contact mode with a

resolution of 1024x1024 pixels at a rate of 3.0 lines/second using a 10 µm scanner.

Images were simultaneously recorded in topography and deflection modes. All images

were acquired in air at room temperature. Gwyddion freeware was used to view and

analyze the images.[35] Roughness parameters for each image were calculated in

Gwyddion after plane flattening. Three images were captured and analyzed for three

independently prepared samples at each protein and mineralization time point

combination (n=9).

2.2.9 Mineral Composition Analysis

Substrate surfaces were demineralized using a modified version of a previously

established procedure.[49] Briefly, mineralized mica-collagen-protein substrates were

demineralized by soaking the sample in 1.0 M nitric acid for 30 minutes. The acid

solution was then neutralized with an equal amount of 1.0 M sodium hydroxide. The

resulting solution from each disc was used in the calcium and phosphate photochemical

assays. Commercial colorimetric assay kits were used to determine the ionic calcium and

phosphate concentrations in the demineralization solutions. The QuantiChrom calcium

assay was used for calcium tests while the PiPer assay was used for determining

phosphate concentrations. Standard calibration curves were constructed for both assay

kits using solutions with known concentrations following the manufacturer's

recommended protocols. The QuantiChrom assay forms a blue colored complex with

calcium via a phenolsulphonephthalein dye. The PiPer assay kit forms resorufin in an

amount proportional to the amount of phosphate present in solution by enzymatic

digestion of sugars, after which the resorufin concentration can be measured

spectrophotometically. Samples were analyzed with a PowerWave XS2 multi-well plate

reader from BioTek (Winooski, VT) at 612 nm and 565 nm for the calcium and

phosphate assays, respectively. Data collection was performed using Gen5 1.07

(BioTek). Ca:P ratios were calculated after determining Ca^{2+} and PO_4^{3-} concentrations

for individual samples. A minimum of 2 samples were analyzed from each of three

independent experiments (n≥7).

2.2.10 Data Analysis

All of the data are presented as the average ± standard error of the mean of all

of the samples for a given data set. The results were identified as being statistically

significant from each other at a 95% confidence interval ($p < 0.05$) using a one-way

analysis of variance (ANOVA) test. The statistical analysis was conducted using OriginPro 8.5 software.

2.3 Results and Discussion

2.3.1 Collagen Substrate Characterization

In order to accurately assess the mineralization induction properties of OPN, BSP, and DPP it is important to conduct the study on a substrate that mimics the native structure of developing bone. Previously it was shown that tropocollagen molecules self-assemble into loosely aligned collagen fibrils on freshly cleaved mica under carefully controlled conditions.[11] This was confirmed in this study by exposing freshly cleaved mica disks to a 0.3 mg/mL solution of collagen in KCl-Tris buffer. Figure 2.1a shows a representative AFM image which clearly demonstrates that a loosely aligned coating of collagen fibrils was obtained with this self-assembly technique. The fibrils exhibited a width of ~100 nm and under higher magnification the prototypical 67 nm *D*-periodicity banding of collagen fibrils was observed (data not shown). Figure 2.1b shows a lower magnification AFM image, to demonstrate the uniformity of this coating across the surface. Figure 1c shows a representative AFM image of the bare mica control surface to clearly demonstrate that the topographical features seen in Figures 2.1 a-b result from the collagen coating. These results indicate that this two dimensional collagen fibril platform is a good *in vitro* analog to developing bone, making it suitable for probing the biomineralization induction properties of the SIBLING proteins. Because the collagen formation procedures were based on previously established methods, no further characterization of the collagen substrate was performed.

2.3.2 Protein Adsorption Isotherms and Freundlich Parameters

In order to compare the effects of the different SIBLING proteins on mineralization, it is important to identify conditions that lead to identical amounts of the proteins being present on the substrate to eliminate the need for normalization. This was accomplished by developing ^{125}I radiolabeled adsorption isotherms for BSP, OPN, and DPP on the collagen-mica substrates. The adsorbed amount of protein was calculated by using the specific measured radioactivity of each protein solution before adsorption and the activity of the collagen-mica substrate after protein adsorption and extensive rinsing. The resulting adsorption isotherms are shown in Figure 2.2. In this Figure it can be observed that BSP has the highest affinity for the collagen-mica substrate at lower exposure concentrations. DPP and OPN had similar binding profiles with DPP having slightly higher adsorption levels at each concentration. However, at the highest exposure concentration of 100 μg/mL, all three proteins converged to a similar amount of specifically adsorbed proteins. These isotherms were then used to determine exposure concentrations that resulted in identical amounts of adsorbed protein for each of the three proteins at an intermediate or lower exposure concentration. A low to intermediate concentration was chosen to better mimic the native concentration of these proteins in bone tissue.[24-26,31] The dotted lines in Figure 2.2 highlight the concentrations that were identified and used in the subsequent mineralization study for each of the three proteins. Specifically, concentrations of 10 μg/mL BSP, 32.5 μg/mL DPP, and 50 μg/mL OPN were used to obtain ~1.3 ng of adsorbed protein per mm^2 of collagen-mica substrate.

The Freundlich adsorption isotherms are shown graphically in Figure 2.3, while the parameters are shown in Table 2.2. As seen in Table 2.2, the K values exhibit a range of 2 order of magnitude with BSP having K=0.001558, DPP having K=0.06574, and OPN having K=0.1825. The high value for OPN is unsurprising given that it has the largest collagen binding constant of the three proteins tested, at 5 μm, and that it binds to multiple areas on the collagen molecule.[23] At low concentrations, such as the ones in this work, BSP and DPP typically localize at the α2 chain of the hole zone and the e-band in the hole zone of collagen, respectively. The n parameters showed the opposite trend with BSP having the highest value n=3.851, DPP having n=3.351, and OPN having the lowest value at n=3.254. Again, the different trend is unsurprising given that the OPN binding domain applies to many regions on the collagen molecule, while BSP and DPP mostly bind to one specific region on a collagen molecule, resulting in a more intense binding interaction between BSP/DPP and collagen at low concentrations.[23]

Following protein adsorption, additional control AFM images were collected to identify topological features that result from protein adsorption. Figure 2.1d shows a representative image for the collagen coated substrates following BSA adsorption. This Figure is representative of all of the substrates following protein adsorption from the three SIBLING proteins as well (data not shown). It can be seen that there are no obvious topological changes as a result of the protein adsorption process. Therefore, it can be concluded that any new topological features seen by AFM following exposure to m-SBF are a mineralization product.

2.3.3 Mineral Morphology Analysis

Following the identification of exposure conditions that resulted in equal amounts of adsorbed BSP, OPN, and DPP, mineralization induction studies were initiated. These studies were conducted by exposing the substrates to Oyane *et al.*'s m-SBF, which closely mimics the native ion concentrations in plasma without the biological components.[48] The subsequent mineralization was characterized following 5, 10, and 24 hours of immersion in the m-SBF. Figures 2.4, 2.5, and 2.6 show representative AFM images for each of the proteins following 5, 10, and 24 hours of mineralization, respectively. Additionally, the average roughness measurements determined from multiple AFM images for each of the protein-time point combinations are summarized in Figure 2.7.

In order to monitor for bulk mineralization effects, control surfaces were completed with heat denatured BSA as a non-mineralizing protein. As seen in Figure 3a, after 5 hours of immersion in m-SBF, the BSA coated surfaces showed some bulk mineralization effects. This is evident when comparing the morphology of the collagen substrate before (Figure 2.1a and 2.1d) and after mineralization. It is more challenging to distinguish the individual fibers following exposure to m-SBF. However, there are no observable changes from the 5 hour time point to the 10 and 24 hour time points as seen in Figures 2.5a and 2.6a. Interestingly, while there are no obvious qualitative differences in the mineralization across the BSA samples there is a difference in the surface roughness across the different time points, including a statistically significant drop off in the roughness following 24 hours of exposure to m-SBF, as compared to 10

hours of exposure. This is shown in Figure 2.7. The likely explanation for these results is that bulk precipitation occurs during the entirety of the m-SBF exposure. Initially bulk precipitation increases the surface roughness, through the 10 hour time point. Beyond that, bulk precipitates may be more likely to settle into features on the sample surface, ultimately leading to a reduction in the surface roughness.

When examining the mineralization on the samples with BSP there were no real qualitative differences that could be observed as compared to the BSA control samples at any of the time points. In Figures 2.4b, 2.5b, and 2.6b it can be seen that there appears to be a minimal degree of mineralization, likely due to precipitation from solution. However, when comparing the quantifiable surface roughness, a different trend from that seen for the BSA controls was seen. In Figure 2.6, it can be seen that there is a drop off in the surface roughness at the 10 hour time point as compared to the 5 and 24 hour time points. However, this difference was not statistically significant and may simply represent sample variability.

The mineralization results seen in the presence of DPP were in stark contrast to the results seen for both BSA and BSP. As seen in Figures 2.4, 2.5c, and 2.6c distinct mineral nodules were seen at all time points on the DPP samples. Furthermore, these mineral nodules appear to correlate well with the collagen fibrils. They also seem to increase slightly in size as the m-SBF exposure time is increased and there does not appear to be a change in the relative number of mineral nodules present as a function of time. The roughness measurements conducted across multiple samples also indicate that there are no significant differences between the samples at any of the time points.

This can be seen in Figure 2.7. These results suggest that there is a uniform

mineralization process occurring on these samples. Additionally, the roughness value is

similar to the maximum values seen with all of the other protein samples. It is believed

that the formation of specific mineral nodules depleted the ion concentration in the

bulk solution, effectively preventing the bulk precipitation believed to occur in the

presence of both BSA and BSP.

The final SIBLING protein that was tested was OPN and representative mineral

morphologies can be seen in Figures 2.4d, 2.5d, and 2.6d. The substrates treated with

OPN appeared to have some mineral formation after 5 hours. It also appears that the

mineral is formed either on top of or alongside the collagen fibrils. As the mineralization

time was increased, these minerals appeared to become less distinct. These

observations correlate with the roughness measurements shown in Figure 2.7. The

roughness was seen to steadily decrease over time. Interestingly, there is no difference

in the surface roughness between the original collagen substrate and the OPN substrate

following 24 hours of exposure to m-SBF. Additionally, this roughness value was

statistically significantly lower than that found following 5 hours of exposure to m-SBF.

These results may suggest that OPN plays a role in the initial surface mineralization, but

that the minerals that are formed mature over time. This would be consistent with the

current perception of OPN's role in biomineralization.

2.3.4 Mineral composition analysis

After characterizing the morphology, surface coverage, and roughness of the

minerals, photochemical assays were used to quantify the amount of calcium and

phosphate ions present under all of the conditions examined above. The complete

demineralization of the samples by the nitric acid procedures was also confirmed by

AFM (data not shown). The absolute concentrations for calcium and phosphate as

determined with this approach can be seen in Figures 2.8a and 2.8b, respectively.

The BSA coated surfaces exhibited a high concentration of calcium relative to the

three SIBLING proteins at 5 and 24 hours as shown in Figure 2.8a. BSA has been shown

to chelate Ca^{2+}, so this result was not unexpected.[50] Interestingly, the relative calcium

concentration following 10 hours of m-SBF exposure showed a significantly lower

amount of Ca^{2+} ions relative to the other time points. This is even more surprising when

combined with the fact that the 10 hour samples had the highest surface roughness of

the BSA samples. There were no differences between the other two time points,

although there was slightly more average calcium present after 5 hours. The phosphate

concentration results showed a similar trend with the greatest measured concentrations

occurring on samples following 5 hours of m-SBF exposure and the lowest

concentrations following 10 hours of exposure.

The measured calcium concentrations from samples with BSP following 5 hours

of exposure to m-SBF were noticeably lower than those seen with BSA. A significant

increase in the amount of calcium was seen at the 10 hour time point, with a nearly

identical amount of calcium present following 24 hours. Both of these points were

statistically greater than the concentration at the 5 hour time point. These maximum

calcium concentrations were similar to those seen in the presence of BSA following 24

hours of exposure to m-SBF and they were the highest measured calcium

concentrations found for minerals formed in the presence of any of the SIBLING

proteins examined in this study. As seen in Figure 2.8b, the phosphate concentrations

from minerals formed in the presence of BSP were relatively constant across all of the

time points examined. There was a slightly lower level at the 10 hour time point, but this

result was not significantly different. There were also no relative differences between

the BSP and BSA samples in terms of the phosphate concentrations.

The calcium and phosphate concentrations found from minerals formed in the

presence of DPP exhibited trends that match what would be expected of a mineralizing

system. If active mineralization was occurring it would be expected that the absolute

concentration of Ca^{2+} and PO_4^{3-} would continually increase over time. The

concentrations of both ions showed continually increasing levels with increased

exposure time only in the presence of DPP. However, it is interesting to note that the

absolute values of the calcium concentrations are noticeably lower than the maximum

measurements for both BSA and BSP. At the same time, the phosphate measurements

at the 10 and 24 hour time points were the highest of any of the SIBLING proteins. These

results are also consistent with the obvious mineral nodule formation seen on the AFM

images. Furthermore, the continual increase in the ion concentrations suggests that the

minerals are either continually growing or they are maturing with increased m-SBF

exposure time.

The relative concentration of calcium in minerals formed in the presence of OPN

also showed a continual increase over time to similar levels as those seen in the

presence of DPP. However, the phosphate concentration levels peaked in the minerals

formed after 10 hours of m-SBF exposure. The amount of phosphate was slightly higher after 24 hours as compared to 5 hours of exposure. It is interesting to consider these results in combination with the roughness results seen in Figure 2.7. The fact that the calcium levels continued to increase with exposure time while the roughness continued to decrease is consistent with the perception that OPN plays a role in mineral maturation.

The final characterization that was conducted was the determination of the calcium to phosphate ratio for individual samples. Calcium phosphate minerals are often identified based on their calcium to phosphate ratio and the mineral component of bone has been seen to have a ratio of approximately 1.49:1.[51] In this study, the Ca:P ratio was determined for the individually demineralized samples using a normalization factor for the calcium concentration. This was necessary because mica is known to contain calcium ions that could be removed during the demineralization process. In order to determine the normalization factor, collagen-mica substrates were prepared, but not exposed to SBF. Then these samples were subjected to the demineralization, calcium assay, and phosphate assay processes. Upon completion, it was found that the collagen-mica substrate produced 7.93 ± 5.08 µmol of calcium (n=5), while there were no detectable levels of phosphate present. This value for calcium was then used to reduce the absolute calcium concentration values before the Ca:P ratio was determined.

The Ca:P ratios of the minerals formed with each of the proteins at each of the time points examined are shown in Figure 2.9. The control BSA sample had a Ca:P ratio trend that was similar to that seen for the Ca^{2+} concentration. Following 5 and 24 hours

27

of m-SBF exposure there were similar Ca:P ratios found, but there was a noticeable

decrease in the ratio measured following 10 hours of exposure. Conversely, in the

presence of all three of the SIBLING proteins, the Ca:P ratio exhibited a peak following

10 hours of m-SBF exposure with the minimum ratio being found following 5 hours of

exposure. There were no statistically significant differences in the maximum values

found for any of the proteins tested. Interestingly, under all of the conditions examined

in this investigation, the Ca:P ratios were much higher than those found in native bone

minerals. This could be due to ion-protein interactions, as all of the SIBLING proteins

have been shown to have strong calcium binding properties.[6,22-24,52] It is also possible

that the high Ca:P ratio could be an indication that immature bone minerals are being

formed. On-going research efforts are focused on determining the crystal state of the

minerals to better understand the SIBLING protein induced biomineralization process

seen under the conditions examined here.

2.4 Conclusions

In this investigation the biomineralization induction properties of three SIBLING

proteins (OPN, BSP, and DPP) were investigated on a biomimetic collagen type I fibril

substrate. The mineralization experiments were conducted under conditions where

identical amounts of adsorbed protein were specifically bound to a loosely aligned

collagen fibril coating. The mineral morphology was characterized using AFM and the

composition was characterized using photochemical assays.   While minerals were

observed in the presence of each of the SIBLING proteins and the control substrate with

adsorbed BSA, only the samples with adsorbed DPP had distinct mineral nodules that

mimic those seen in developing bone. Furthermore, all of the minerals found under the conditions used in this investigation had Ca:P ratios that were significantly larger than what has been found in native bone tissue. When taken together, these results suggest that the SIBLING proteins can mediate the biomineralization process. However, it is likely that the minerals mature over a longer period of time that what was examined in this study or following exposure to a second SIBLING protein.

2.5 List of Figures and Tables

Table 2.1- Preparation conditions for 500 mL of SBF using Oyane *et al.*'s recipe for m-SBF.[48]

Reagent	Quantity (g)
NaCl	2.7015
NaHCO$_3$	0.252
Na$_2$CO$_3$	0.213
KCl	0.1125
K$_2$HPO$_4$	0.115
MgCl$_2$·6H$_2$O	0.1555
HEPES[a]	8.946[b]
CaCl$_2$	0.1465
Na$_2$SO$_4$	0.036
1.0 M NaOH	[c]

[a] 2-(4-(2-hydroxyethyl)-1-piperazinyl)ethanesulfonic acid.
[b] HEPES was dissolved in 50 mL of 0.2 M NaOH before addition
[c] Added until pH 7.4.
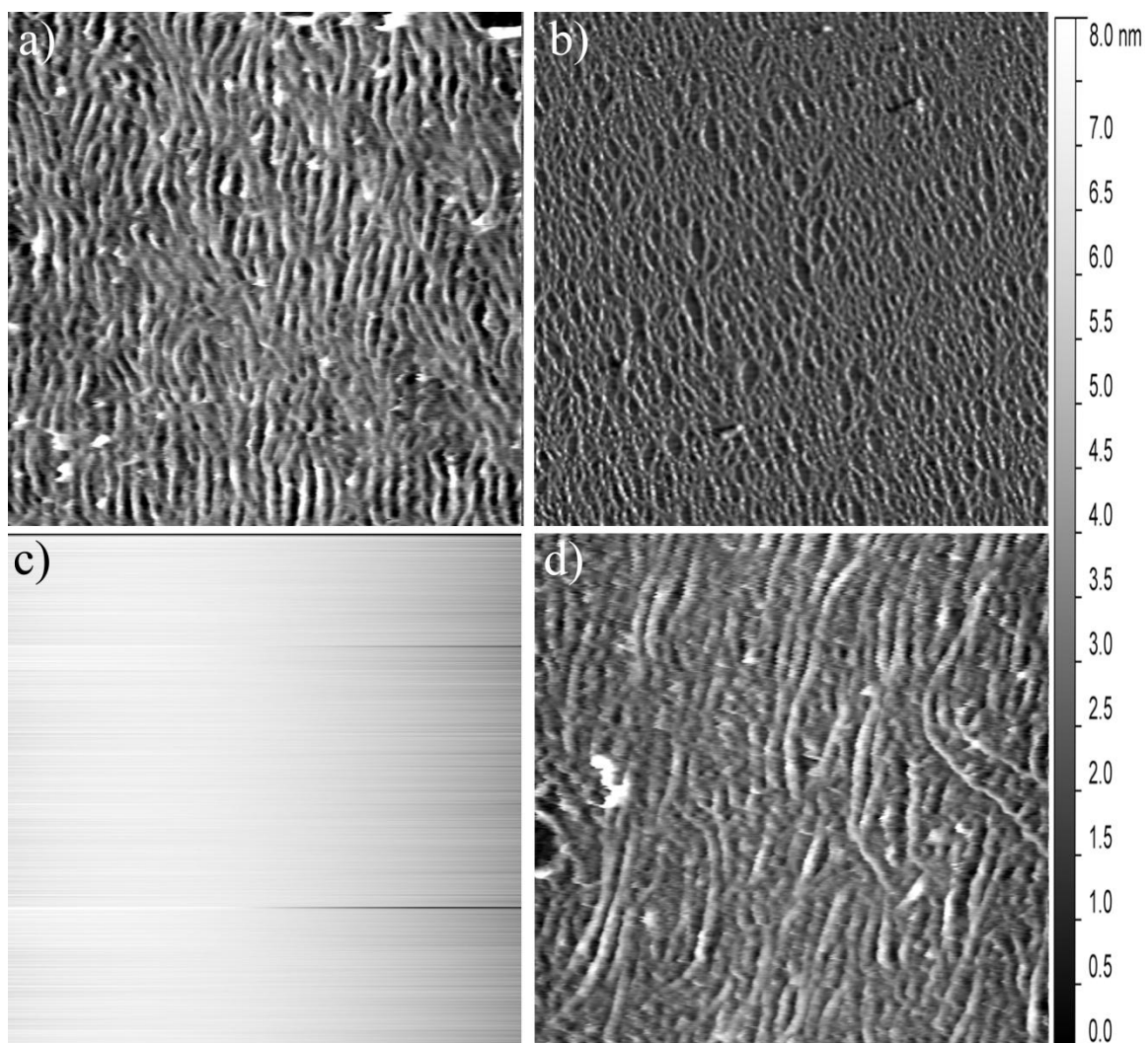
Figure 2.1 – Representative AFM images showing a) a 2.5 μm x 2.5 μm section of the collagen-mica substrate and b) a 10 μm x 10 μm section of the collagen-mica substrate, both following the self-assembly of a coating of loosely aligned collagen fibrils; c) a 2.5 μm x 2.5 μm section of the bare mica substrate before collagen fibril assembly; and d) 2.5 μm x 2.5 μm section of the collage-mica substrate following exposure to 1 mg/mL of heat denatured BSA.
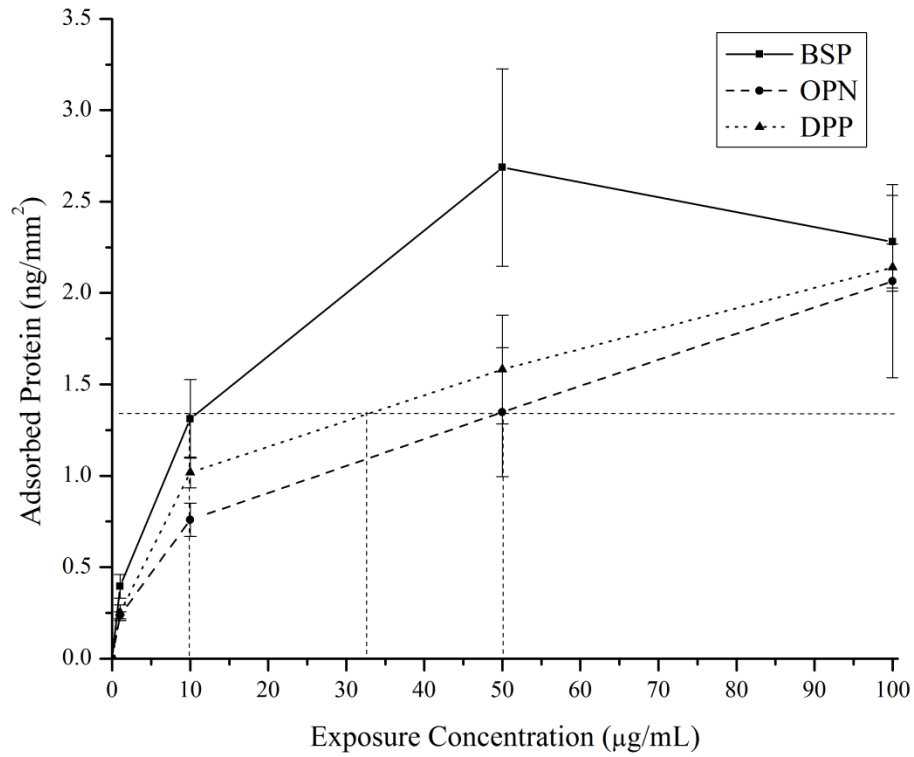
Figure 2.2 – [125]I radiolabeled adsorption isotherms for BSP (squares), OPN (circles), and DPP (triangles) on the collagen-mica substrate. The dotted lines indicate the exposure concentrations used for each of the three proteins in the subsequent mineralization studies. The data is presented as the mean ± standard error of the mean from three independently prepared samples (n=3).

Table 2.2 – K, n, and R^2 parameters for BSP, DPP, and OPN derived from applying the Freundlich equation to the ^{125}I radiolabeled SIBLING adsorption isotherm.

Protein	K	n	R^2
BSP	0.001558	3.851	0.7907
DPP	0.06574	3.351	0.8755
OPN	0.1825	3.254	0.9446
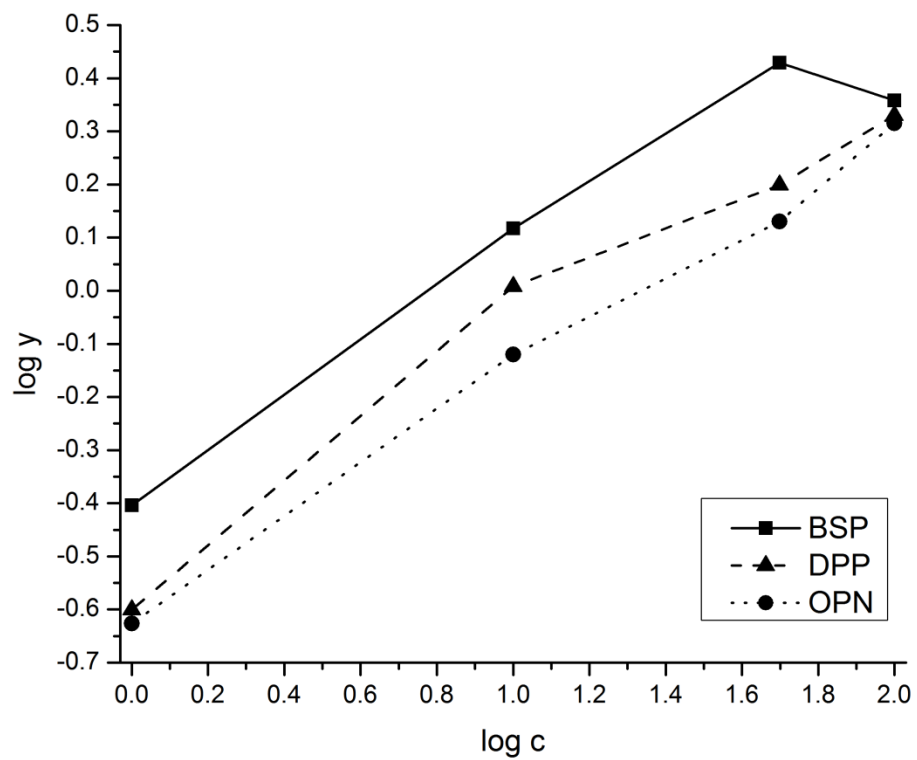
Figure 2.3 –Freundlich adsorption isotherms resulting from the ^{125}I radiolabeled adsorption isotherms for BSP (squares), OPN (circles), and DPP (triangles). The data is presented as the mean from three independently prepared samples (n=3).
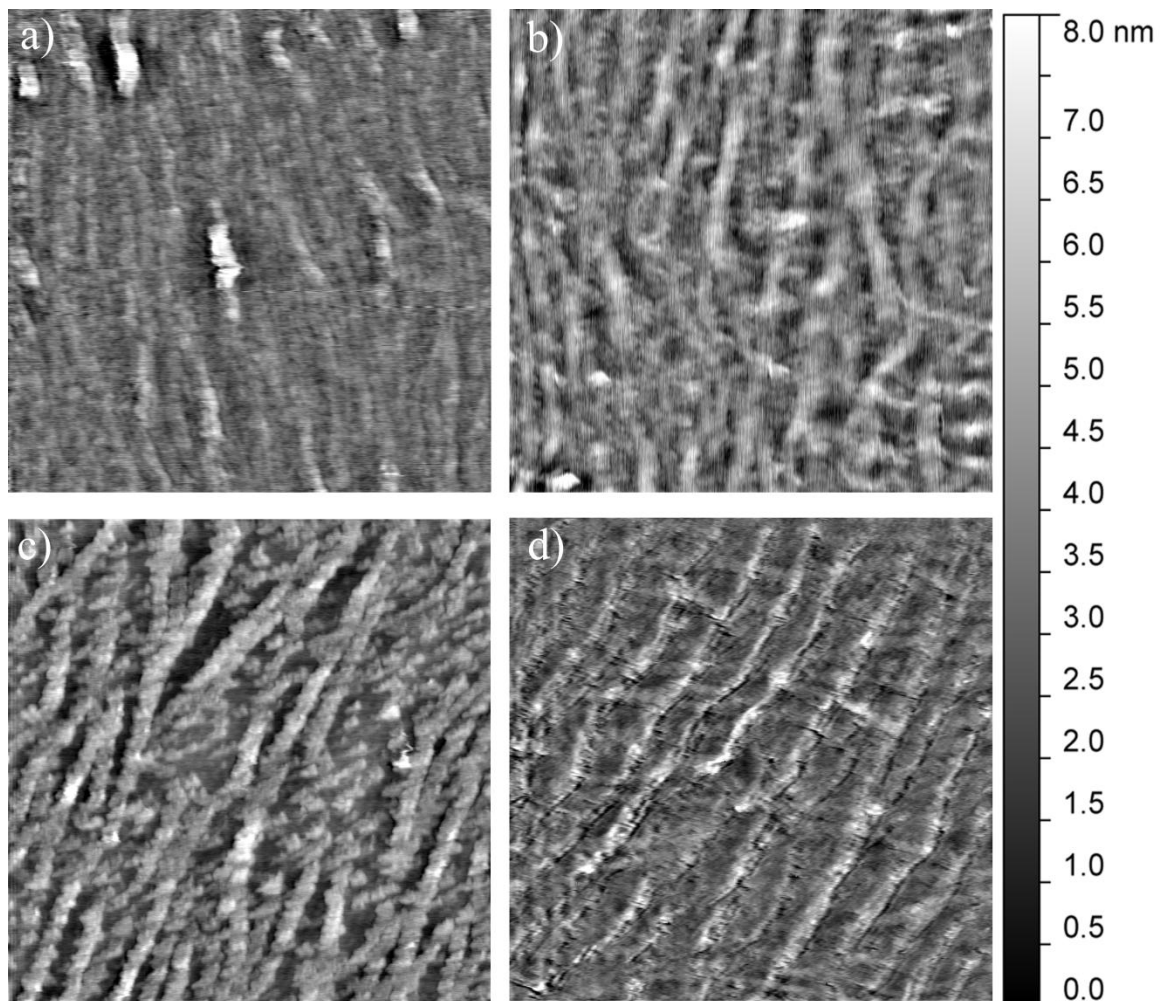
Figure 2.4 – Representative 2.5 µm x 2.5 µm AFM images of the mineralization induced on the collagen-mica substrate after 5 hours of immersion in SBF in the presence of (a) 1 mg/mL heat denatured BSA, (b) 10 µg/mL BSP, (c) 35.5 µg/mL DPP, and (d) 50 µg/mL OPN.
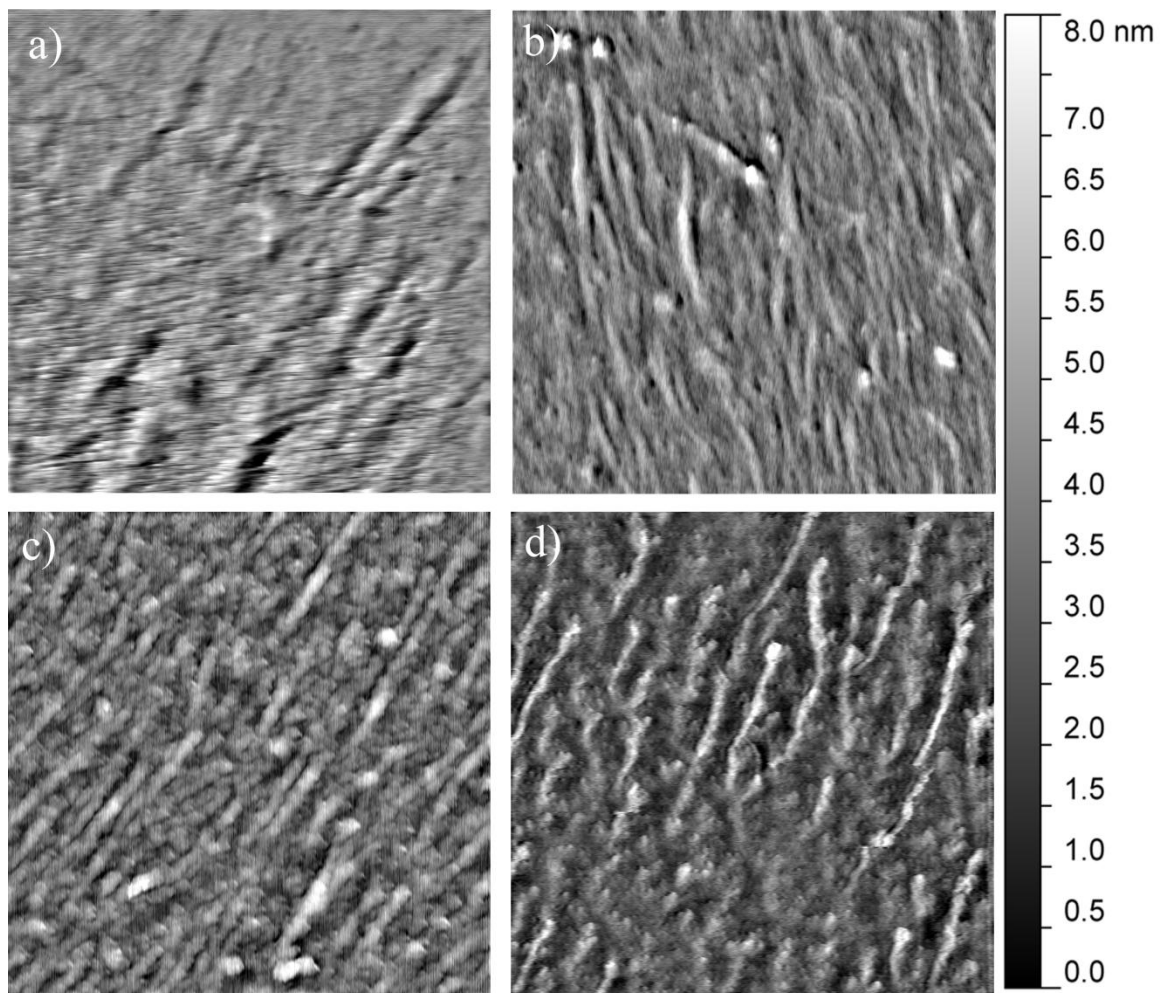
Figure 2.5 – Representative 2.5 μm x 2.5 μm AFM images of the mineralization induced on the collagen-mica substrate after 10 hours of immersion in SBF in the presence of (a) 1 mg/mL heat denatured BSA, (b) 10 μg/mL BSP, (c) 35.5 μg/mL DPP, and (d) 50 μg/mL OPN.
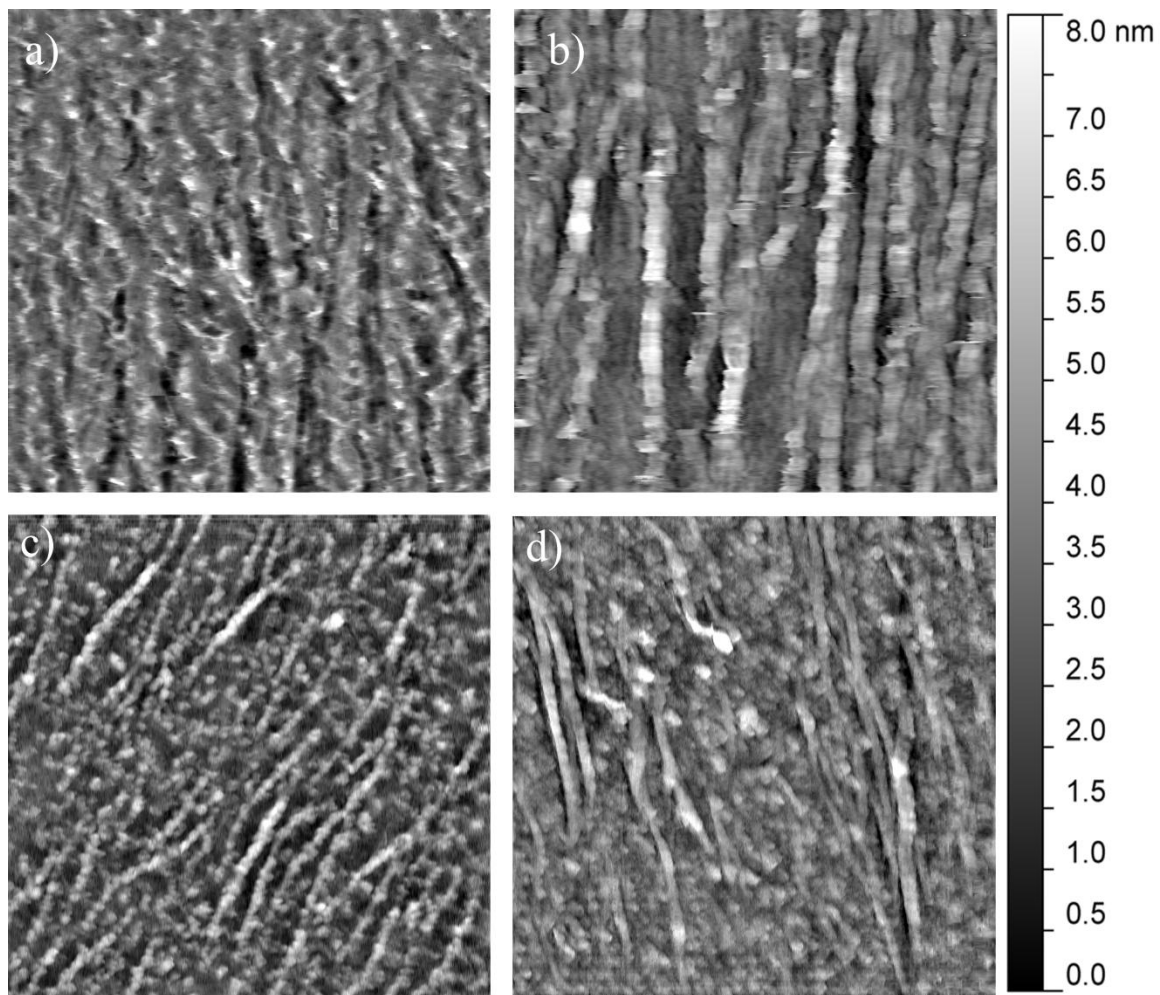
Figure 2.6 – Representative 2.5 μm x 2.5 μm AFM images of the mineralization induced on the collagen-mica substrate after 24 hours of immersion in SBF in the presence of (a) 1 mg/mL heat denatured BSA, (b) 10 μg/mL BSP, (c) 35.5 μg/mL DPP, and (d) 50 μg/mL OPN.
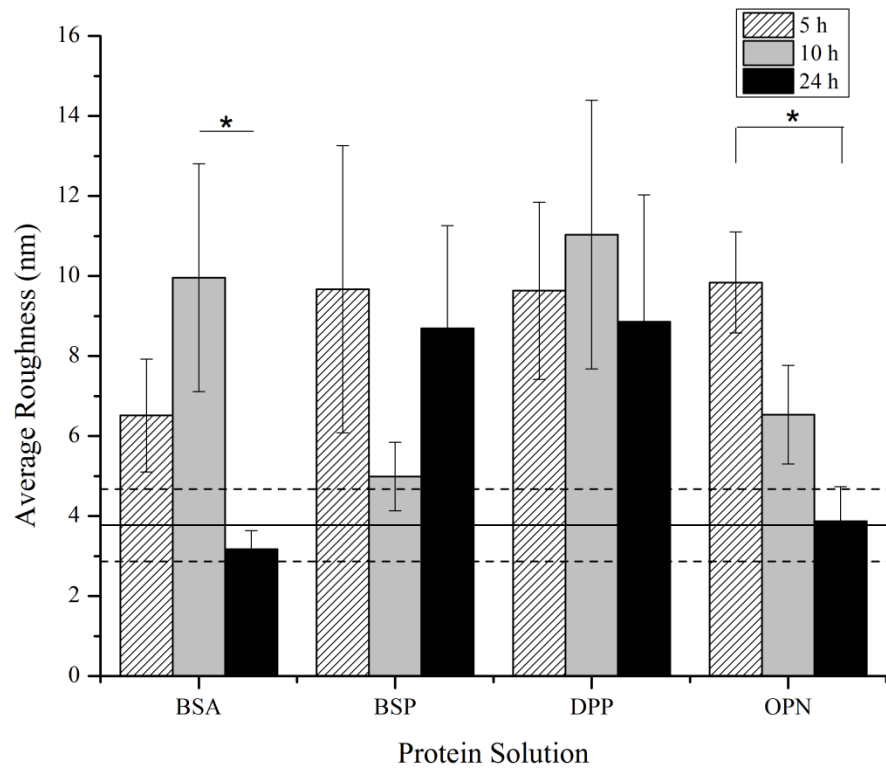
Figure 2.7 - Mean ± standard error of the mean of the surface roughness of the mineralized substrates after immersion in SBF for 5, 10, and 24 hours in the presence of proteins (n=9). The solid horizontal line represents the average roughness of the original collagen substrate prior to protein adsorption and mineralization and the dashed lines represent the standard error of the mean for this control. A * represents a statistically significant difference between the surfaces being compared at a 95% confidence interval ($p < 0.05$).
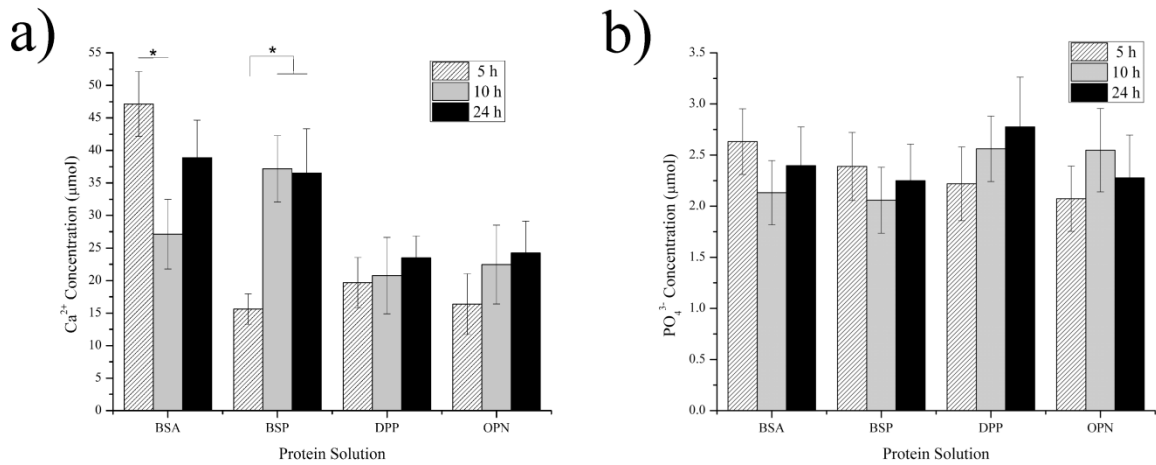
Figure 2.8 – Mean ± standard error of the mean of the measured (a) Ca^{2+} and (b) PO_4^{3-} concentrations following the demineralization of the collagen-mica substrates after immersion in SBF for 5, 10, and 24 hours in the presence of adsorbed BSA, BSP, DPP, or OPN. The concentrations were determined using calcium and phosphate assay kits for a minimum of 7 independently prepared samples (n≥7). A * represents a statistically significant difference between the surfaces being compared at a 95% confidence interval ($p < 0.05$).
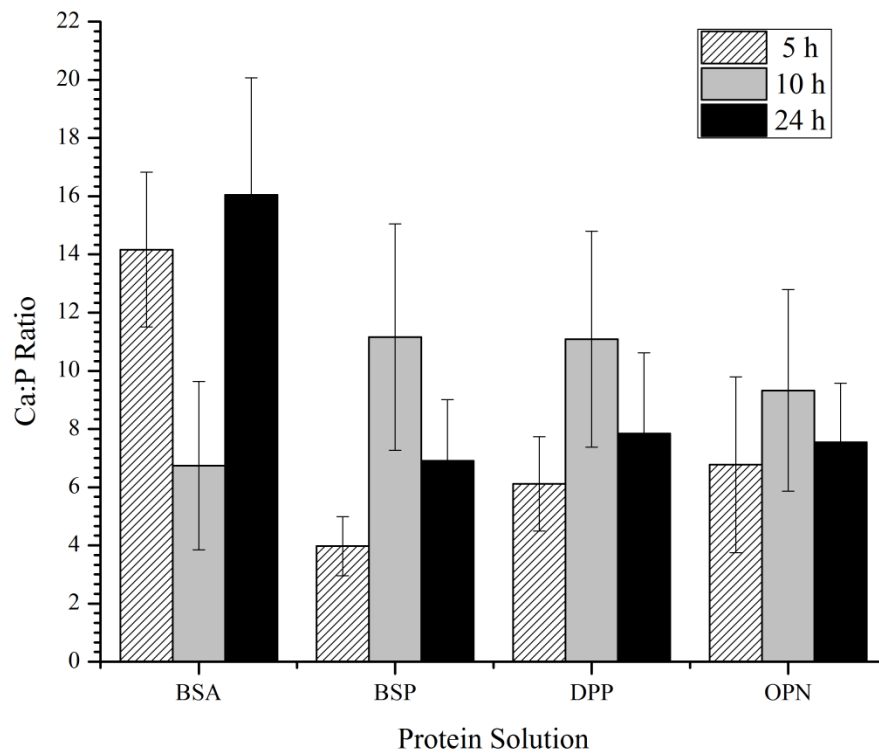
Figure 2.9 – Mean ± standard error of the mean of the normalized Ca:P ratio following the demineralization of the collagen-mica substrates after immersion in SBF for 5, 10, and 24 hours in the presence of adsorbed BSA, BSP, DPP, or OPN. The ratio for a minimum of 5 independently prepared samples were determined under each condition (n>5).

CHAPTER 3. Adhesion of MC3T3-E1 cells bound to dentin phosphoprotein specifically bound to collagen type-I

The following chapter was first published in a similar form in the Journal of Biomedical

Materials Research, Part A and can be located using the following information:

Zurick Kevin M., Qin C, Bernards MT. 2012. Adhesion of MC3T3-E1 cells bound to dentin phosphoprotein specifically bound to collagen type I. J Biomed Mater Res Part A 2012:100A:2492–2498.

3.1 Introduction

In this investigation, DPP is studied to better formalize the role that this protein plays aiding cellular adhesion to the ECM of developing bone. Previous work has examined MC3T3-E1 osteoblast-like cell binding onto surfaces covered with either OPN or BSP when the proteins were either oriented through specific binding interactions with collagen or randomly adsorbed onto tissue culture polystyrene (TCPS) substrates. A statistically significant difference was detected in the amount of cell binding on the collagen-OPN surfaces, indicating a preferential orientation and/or conformation for MC3T3-E1 cell adhesion when OPN was specifically bound to collagen.[34] In this investigation OPN, BSP, and DPP are studied to better formalize the individual roles that these proteins play in biomineralization.

The foci of this work are to (a) probe the natural orientation of DPP with respect to its cell binding domain when it is specifically bound to collagen or randomly adsorbed to TCPS and (b) compare the overall cell binding capabilities of DPP to previous work with OPN[34] and BSP.[29] This study provides valuable insight into the relative importance of DPP for promoting cellular adhesion to the collagen matrix of developing bone. While performing this study, it was important to ensure that there were identical amounts of DPP bound to both the TCPS and collagen substrates. This was accomplished by developing ^{125}I radiolabeled adsorption isotherms that were subsequently used to determine DPP exposure concentrations that would result in equal amounts of adsorbed protein on the two substrates. Cell adhesion assays were conducted with MC3T3-E1 osteoblast-like cells and inhibition assays were performed with a GRGDSP peptide to

confirm that the cell adhesion was due to integrin interactions with the RGD sequence of DPP. In this study it was found that DPP does not have a favorable orientation for promoting cell binding when specifically bound to collagen. This suggests that DPP does not play a major role in promoting cellular adhesion to the matrix of developing bone.

3.2 Experimental Procedures

3.2.1 Materials

Ultrapure water (18.2 MΩ-cm) was obtained from a Millipore Synergy UV water purification system (Billerica, MA) and was used for all experiments. Tissue culture polystyrene (TCPS) flasks were purchased from Corning (Corning, NY). To obtain TCPS substrates, sterile flasks were scored into 5x5 mm squares with a drill press and broken apart prior to use in experiments. NaCl and tris(hydroxymethyl)aminomethane (Tris-HCl) were purchased from Thermo Fisher Scientific (Waltham, MA). NaCl-Tris buffer was prepared by dissolving 25 mM Tris-HCl (Fisher Scientific, Fair Lawn, NJ) and 125 mM NaCl in 18.2 MΩ-cm water and adjusting the pH to 7.4 with 1.0 M NaOH (Sigma). Type I collagen from rat tail with a purity of >90% was purchased from BD Biosciences (Bedford, MA). Bovine serum albumin (BSA) with a purity of >96% was purchased from Sigma-Aldrich (Saint Louis, MO). Heat denatured BSA was prepared by dissolving 1 mg/mL of BSA in NaCl-Tris buffer and heating at 60 ^{o}C for 30 minutes. A 4% paraformaldehyde solution was made by dissolving paraformaldehyde (Thermo-Fisher Scientific) in pH 7.4 phosphate buffered saline (PBS, Sigma-Aldrich, Saint Louis, MO) at 60 ^{o}C until the solution became clear. Hematoxilin was purchased from Acros Organics (Geel, Belgium). A soluble GRGDSP peptide was purchased from Calbiochem (La Jolla,

CA). All other cell culture supplies, including fetal bovine serum, α-minimum essential medium (α-MEM), penicillin-streptomycin, trypsin-ethylenediaminetetraacetic acid (trypsin-EDTA, 0.05%, 0.53 mM), and soybean trypsin inhibitor were purchased from Invitrogen (Carlsbad, CA). All buffer solutions and cell culture media were filter sterilized with 0.22 μm vacuum filters and stored at 4 ^{o}C prior to use. MC3T3-E1 osteoblast-like cells (subclone 14, ATCC# CRL-2594) were obtained from ATCC (Manassas, VA).

3.2.2 Substrate Preparation

Collagen-TCPS and TCPS substrates were prepared using previously established procedures. Briefly, TCPS squares were incubated in 1 mL of NaCl-Tris buffer overnight at room temperature. Afterward, they were rinsed extensively with 18.2 MΩ-cm water and dried with filtered air before being used immediately in subsequent experiments. Collagen-TCPS substrates were prepared by soaking TCPS squares in 1 mL of a 50 μg/mL collagen in NaCl-Tris buffer overnight at room temperature. Following this, the substrates were removed from the collagen solution, rinsed extensively with 18.2 MΩ-cm water, dried with filtered air, and then soaked in 1 mL of 1 mg/mL heat denatured BSA for 5 hours to block nonspecific protein binding to any exposed TCPS. Afterwards, the TCPS-collagen substrates were rinsed with 18.2 MΩ-cm water, dried with filtered air, and then used immediately in subsequent experiments.

3.2.3 Dentin Phosphoprotein Isolation

The noncollagenous proteins including DPP were extracted and isolated from the incisor dentin of 10-week-old rats by standard procedures as described earlier.[45,46] For the separation of noncollagenous proteins including DPP, the rat dentin extracts were

first passed through a Sephacryl S-200 (Amersham Biosciences, Little Chalfont, Buckinghamshire, UK) gel chromatography column.[46] The Sephacryl S-200 column separated noncollagenous proteins into four major fractions, and an earlier fraction known as ES1 contained a group of higher molecular weight proteins. The ES1 fraction (containing DPP) was loaded onto a Q-Sepharose (Amersham Biosciences, Piscataway, NJ) ion-exchange column connected to a fast-protein liquid chromatography system, and it was eluted within a gradient ranging from 0.1 to 0.8 M NaCl in 6 M urea (pH 7.4). Then, the fractions enriched with DPP were passed through a Bio-Gel A50m size exclusion column (Bio-Rad, Hercules, CA). The fractions from the Bio-Gel A50m column that contained the most highly pure DPP were combined, dialyzed against water, lyophilized, and used for this study.

3.2.4 Protein Adsorption Isotherms

DPP was labeled with ^{125}I using iodogen reagent and a modified version of a previously published procedure.[47] Briefly, 100 μg of iodogen was suspended in 35 μL of 1.5 mg/mL DPP in ultrapure water, to which 750 μCi of ^{125}I-Na (100 mCi/mL) was added. After 5 min, the mixture was transferred to a 20 cm Sephadex G25-150 column that had been equilibrated with PBS (pH 7.4). The column was then eluted with 15 mL of PBS and 500 μL fractions were collected. The radioactivity associated with each fraction was determined, and the highest count radiolabeled fraction was selected and used in all adsorption isotherm experiments.

[125]I radiolabeled DPP was added to 1.0 mg/mL solutions of unlabeled DPP to obtain solutions with a specific activity of 116.0 counts per minute (cpm) per nanogram

of protein. TCPS and collagen-coated TCPS were prepared as described above. Following

the buffer soak (TCPS) or heat denatured BSA soak (TCPS-collagen), the substrates were

extensively rinsed with 18.2 MΩ-cm water and then incubated with 1, 10, 50, and 100

µg/mL DPP overnight at 4 $^{\circ}$C in a humidified atmosphere. Afterwards, they were rinsed

3 times with NaCl-Tris buffer to remove loosely adsorbed proteins. The cpm

radioactivity of all samples was measured by a Wizard 1470 automatic gamma counter

(PerkinElmer, Waltham, MA). The amount of protein specifically adsorbed to the surface

of the substrates was calculated by relating the cpm of each sample to the sample

surface area and specific activity of the original DPP protein mixture. Each exposure

concentration and substrate combination was repeated three times and the data are

presented as the mean ± standard deviation of these trials.

3.2.5 Cell Culture

MC3T3-E1 cells were continuously grown on TCPS flasks in α-MEM which was

supplemented with a 1% penicillin-streptomycin solution and 10% fetal bovine serum in

a humidified atmosphere at 37 $^{\circ}$C and 5% CO_2. To passage, the cells were rinsed twice

with 10 mL of NaCl-Tris buffer followed by incubation in 2 mL of trypsin-EDTA. After the

cells detached from the flask wall, they were resuspended in supplemented α-MEM and

replated into new TCPS flasks. The cells were passaged once a week and passages 5–10

were used for experiments.

3.2.6 Cell Adhesion Assay

The cell adhesion assay is similar to that used previously to examine the

orientation of proteins specifically bound to collagen.[29,34] TCPS and collagen-coated

TCPS squares were prepared as described earlier. The protein adsorption steps were identical to those performed in the adsorption isotherm experiment, with the exception that only one concentration was used for each type of substrate and only native, unlabeled protein was used. TCPS substrates were exposed to 32.5 µg/mL of DPP while TCPS-collagen substrates were exposed to 50 µg/mL of DPP. Substrates were incubated overnight in a humidified atmosphere at 4 ^{o}C. Following the overnight adsorption, substrates were placed in a 24-well culture plate where they were rinsed 3 times with 1 mL of NaCl-Tris buffer and then blocked with 1 mL of 1 mg/mL heat denatured BSA for 30 minutes. In the meantime, freshly confluent MC3T3-E1 cells were detached with 2 mL of trypsin-EDTA and resuspended in 5 mL of 5 mg/mL soybean trypsin inhibitor in PBS at pH 7.4. The cells were then centrifuged for 5 minutes at 1000 rpm, after which the supernatant was removed and the cells were washed two times with 10 mL of 5 mg/mL BSA in serum free α-MEM. Following this, the cells were resuspended in serum free α-MEM and diluted to a final concentration of 1×10^{5} cells/mL, as determined with a hemocytometer. The cells were incubated for 15 minutes in α-MEM before use in the cell adhesion assay. After the BSA blocking of the well plates was complete, the BSA was removed from the wells and the samples were rinsed three times with 1 mL of NaCl-Tris buffer. Following the rinsing step, 1 mL of cell solution was added to each well and the well plates were incubated for 2 hours in a humidified atmosphere with 5% CO_2 at 37 ^{o}C. Three samples of each substrate type were prepared for each assay and the assay was performed three times.

3.2.7 Cell Binding Inhibition Assay

The cell inhibition assay was performed in a similar fashion to the cell adhesion assay, with one exception. Before the addition of the dilute cells to the samples, the cells were first incubated with 1 mM of a soluble GRGDSP peptide in α-MEM for 15 minutes.[53] This incubation step replaced the final cell incubation step in the adhesion assay procedures. Three substrates were prepared for each assay, and the assay was performed three times.

3.2.8 Cell Fixation and Staining

After the cell adhesion and inhibition assays, the cell solution was removed from the wells and the wells were washed three times with warm (37 $^{\circ}$C) NaCl-Tris buffer to remove loosely bound cells. After this, the cells were fixed by adding 1 mL of 4% paraformaldehyde to each well for 5 minutes. The samples were then rinsed three times with 1 mL of warm NaCl-Tris buffer and then stained with 1 mL of hematoxilin for 5 minutes. Next, the samples were rinsed extensively with ultrapure water and exposed to 1 mL of warm NaCl-Tris buffer for 3 minutes. The samples were then rinsed three times with ultrapure water and dried in air. Three 10X brightfield images from each sample were randomly selected and captured using a Nikon Eclipse Ti optical microscope (Shinjuku, Tokyo, Japan) equipped with a Nikon DS-2MBW camera and NIS Elements – BR 3.1 software (Nikon).

3.2.9 Data Analysis

The number of adherent cells was used to compare the response of the MC3T3-E1 cells to the two substrate-DPP combinations. The total number of cells that adhered

to each sample were physically counted using NIS Elements – BR 3.1 software from each of the images that were captured. A total of 27 images from 9 independently prepared samples were analyzed for each protein-substrate combination. The sample data are presented as the average of all the images obtained and the error bars represent the standard error of the mean (SE). Sample results were analyzed using one-way analysis of variance (ANOVA) and they were considered statistically significant when they had a probability value less than 0.05 ($p < 0.05$). Statistical analysis was performed using OriginPro 8.5 (OriginLab Corporation, MA).

3.3 Results and Discussion

The high purity of the DPP used in this study was confirmed with polyacrylamide gel electrophoresis (SDS-PAGE) using 5 ± 15% gradient gels and Stains-All staining.[46] The results shown in Figure 3.1 show that the rat dentin DPP used in this study migrated between the 83 and 115 kDa molecular weight markers. This is consistent with the migration rate of rat DPP as reported by Butler et al.[54]

To properly compare the orientation and/or conformation of DPP specifically bound to collagen with respect to its cell binding capabilities, it is important to have identical amounts of protein adsorbed to all of the substrates under comparison. This was accomplished by developing ^{125}I radiolabeled adsorption isotherms for DPP on collagen-TCPS and untreated TCPS. The adsorbed amount of protein was calculated by using the specific measured radioactivity of each protein solution before adsorption and the activity of the TCPS or collagen-TCPS substrate after protein adsorption and extensive rinsing. The resulting adsorption isotherms are shown in Figure 3.2 and

confirm that DPP was adsorbed to the TCPS substrates and specifically bound to collagen on the collagen-TCPS substrates. In this figure it can be observed that DPP exhibited a higher affinity for untreated TCPS at exposure concentrations of 50 and 100 μg/mL, while more protein was absorbed on the collagen TCPS at concentrations of 1 and 10 μg/mL. It is expected that DPP would adsorb more readily to the TCPS substrate, especially at higher concentrations, because of differences in the number of binding domains available on the two substrates. This trend was similar to that seen in previous related studies with OPN and BSP.[29,34] It should be noted that total amount of adsorbed protein amounts is higher in this study than corresponding studies with OPN and BSP, confirming that DPP has a strong affinity for collagen.[20,29,34] The isotherms were used to determine concentrations that would result in identical amounts of adsorbed protein on both substrates. Specifically, an exposure concentration of 50 μg/mL DPP was used on the collagen-TCPS substrate and 32.5 μg/mL DPP was used on the TCPS control in subsequent cell binding experiments. The presence of identical amounts of protein on each of the substrates allows for direct comparisons of the two substrates tested without the need for data normalization.

After establishing DPP concentrations that resulted in identical amounts of adhered protein on both substrates, cell binding assays were performed in order to probe the orientation and/or conformation of DPP with respect to its cell binding domain when specifically bound to collagen type I. Because there are no specific binding interactions between DPP and TCPS, this substrate demonstrates the accessibility of the cell binding sequence when DPP has a random orientation or conformation. At the same

time, DPP is known to have a specific binding interaction with collagen. Therefore, the substrate should demonstrate the native orientation or conformation of DPP when specifically bound to collagen. Similar studies have been performed for OPN and BSP.[29,34] In these previous studies, it was found that OPN has a positive orientation for cell binding when specifically bound to collagen while the cell binding properties of BSP appear to be mediated by the conformational flexibility of the protein.[29]

Figures 3.3 a-b show representative light microscopy images of the cell binding to both TCPS and collagen-TCPS in the presence of DPP. In these images it can be seen that there is a slight preference for cell binding to the TCPS substrate when compared to the collagen-TCPS substrate. This suggests that the specific binding interactions between collagen and DPP lead to a negative or unfavorable orientation and/or conformation of DPP for cell binding. Figure 3.3 c-d show representative light microscopy images from the cell inhibition assay for both substrates in the presence of DPP. The fact that all cell binding is essentially eliminated when the cells are exposed to the GRGDSP peptide confirms that the cell binding seen in Figure 3.3 a-b is through cell integrin interactions with the RGD sequence of DPP. To confirm that the differences in the cell binding are not caused by the different underlying substrates, control studies were conducted with heat denatured BSA. Representative light microscopy images for these controls can be seen in Figure 3.4 a-b. These images confirm that the differences in the level of bound cells are due to differences in the accessibility of the RGD sequence and not the underlying substrate composition. This is further supported by the quantitative analysis completed over multiple images and independently prepared

samples. These results are shown in Figure 3.5. In this figure it can be seen that there is

a two to three fold increase in the number of adherent cells in the presence of DPP as

compared to the BSA controls. Additionally, there are ~40% more cells bound to the

TCPS control as compared to the collagen-TCPS substrate in the presence of DPP. This

difference was also determined to be statistically significant (p=0.015).

These results demonstrate that the RGD cell binding sequence in DPP is less

accessible when the protein is specifically bound to collagen. Further insight into the

role of conformation versus orientation can be gained by comparing the results of this

study to those obtained previously with both OPN and BSP.[29] OPN was found to have a

favorable orientation for cell binding because it had an intermediate amount of bound

cells when randomly oriented on TCPS and a nearly confluent coverage of cells when

bound to collagen-TCPS. Alternatively, the cell binding properties of BSP were found to

be dictated by its conformational flexibility because there was nearly confluent coverage

of cells on both substrates. If the cell binding properties of DPP were dictated by

conformational flexibility, it would be expected that a nearly confluent layer of bound

cells would be obtained with the TCPS control substrate. Rather, an intermediate

surface coverage was found, similar to OPN. In addition, the cell adhesion results

obtained with BSP had no statistically significant difference between the two substrates,

indicating an equal accessibility to the RGD sequence. This was not the case with OPN or

DPP. While the binding interaction between OPN and collagen lead to a threefold

increase in the number of adherent cells suggesting a positive orientation for cell

binding, the amount of adherent cells in the presence of DPP was reduced when the

protein was bound to collagen, suggesting a negative orientation for cell binding. The results obtained in this study, when combined with the related work, indicated that there is an orientation dependence of DPP with regard to its cell binding properties.

An important feature of DPP is the large number of aspartic acid-serine-serine (DSS) repeats throughout the amino acid sequence. These DSS repeats are highly negative and are believed to play a role in Ca^{2+} chelation and subsequent mineral formation. In addition, DPP has been shown to adopt a more sheet like structure calcium has been bound to these DSS sequences.[23] Given these properties, it is possible that DPP plays a role in cell binding to the mineral matrix of developing bone rather than the collagen matrix. Previously it was demonstrated that OPN has a negative orientation for cell binding to a hydroxyapatite matrix.[33] When combined with the results obtained in this study, it is possible that DPP could play the opposite role and this work is currently under investigation.

3.4 Conclusions

In this study, DPP adsorption isotherms were obtained on both TCPS and collagen coated TCPS substrates by radiolabeling. These isotherms were then used to identify conditions that lead to identical amounts of adsorbed proteins for use in subsequent MC3T3-E1 cellular adhesion assays to gain insight into the conformation and/or orientation imparted to DPP based on its specific binding interactions with collagen. It was shown that there were significantly lower levels of cell adhesion when DPP was specifically bound to collagen I as compared to the TCPS control. There were also noticeably fewer adherent cells in the presence of DPP as compared to previous

studies with OPN [34] and BSP,[29] even though there were greater amounts of protein present. This suggests that DPP does not play a role in cellular adhesion to the collagen matrix of developing bone.

3.5 List of Figures
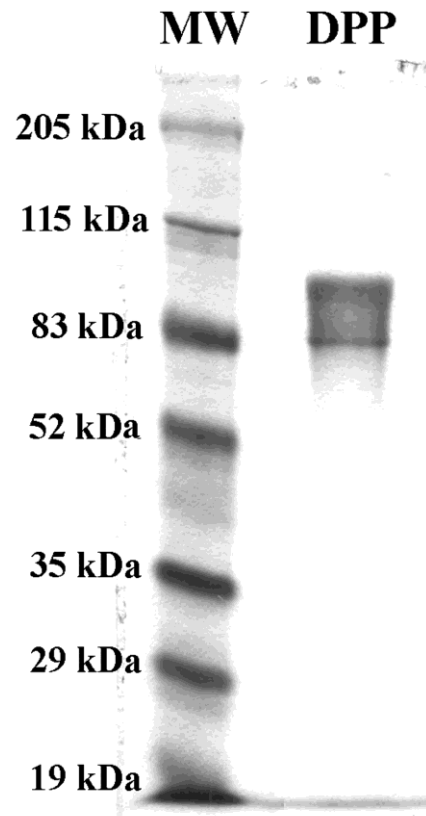
Figure 3.1: SDS-PAGE and Stains-All staining of DPP isolated from rat dentin incisors. Two micrograms of DPP were loaded onto 5–15% gradient gel. The gel was stained with Stains-All. Note the high purity of DPP.
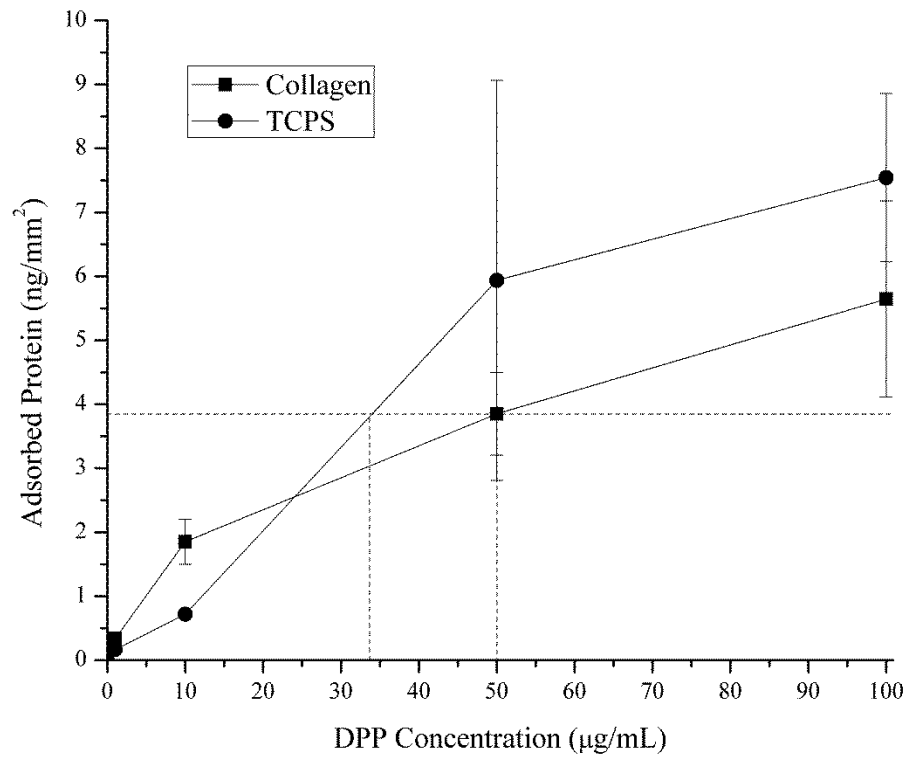
Figure 3.2: [125]I radiolabeled adsorption isotherms for DPP on TCPS (circles) and collagen coated TCPS (squares). The dotted lines represent the concentrations used in the cell adhesion and inhibition assays. The data are shown as the mean ± standard deviation (n=3).
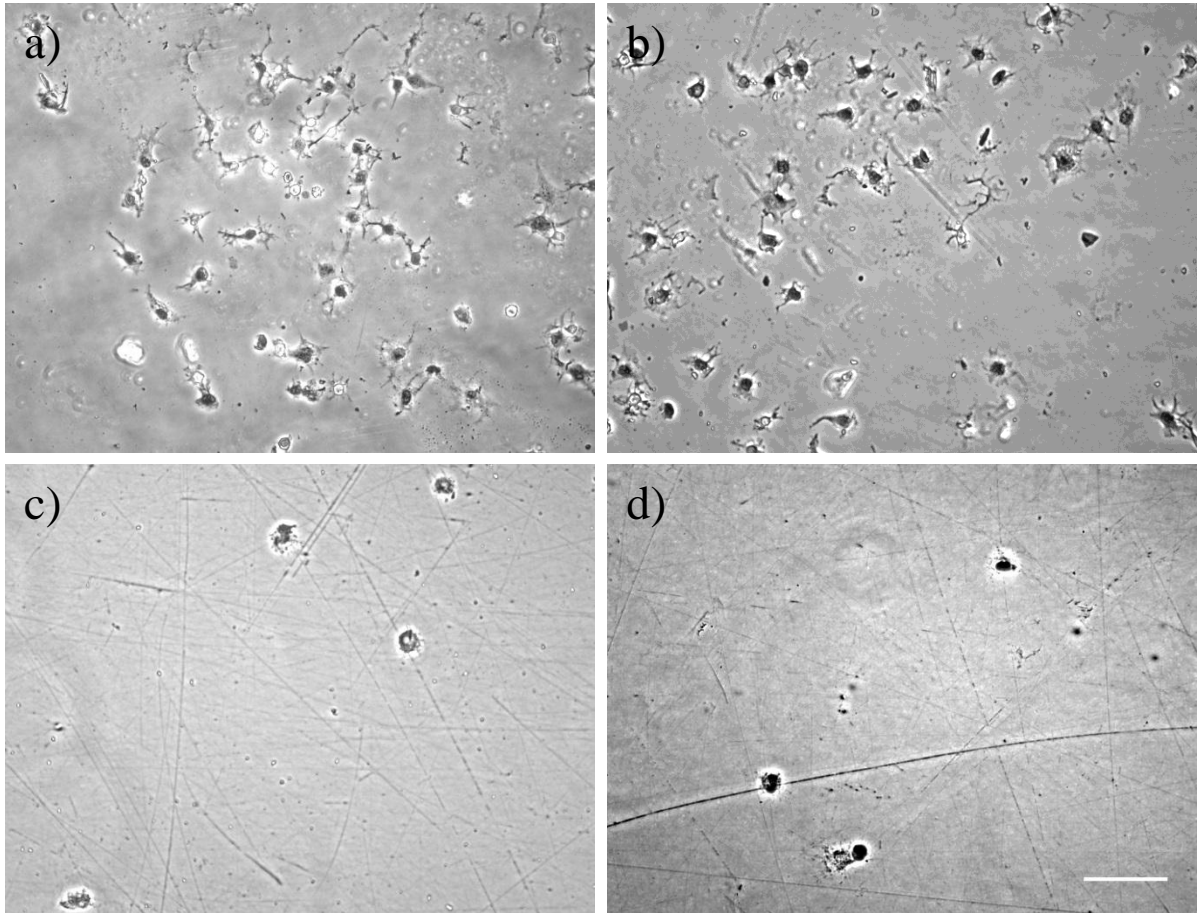
Figure 3.3: Optical microscopy images of MC3T3-E1 cell adhesion on different substrates: (a) 32.5 µg/mL DPP adsorbed on TCPS (b) 50 µg/mL DPP adsorbed to collagen coated TCPS (c) 32.5 µg/mL DPP adsorbed on TCPS in the presence of 1.0 mM GRGDSP (d) 50 µg/mL DPP adsorbed to collagen coated TCPS in the presence of 1.0 mM GRGDSP. The scale bar represents 100 µm.
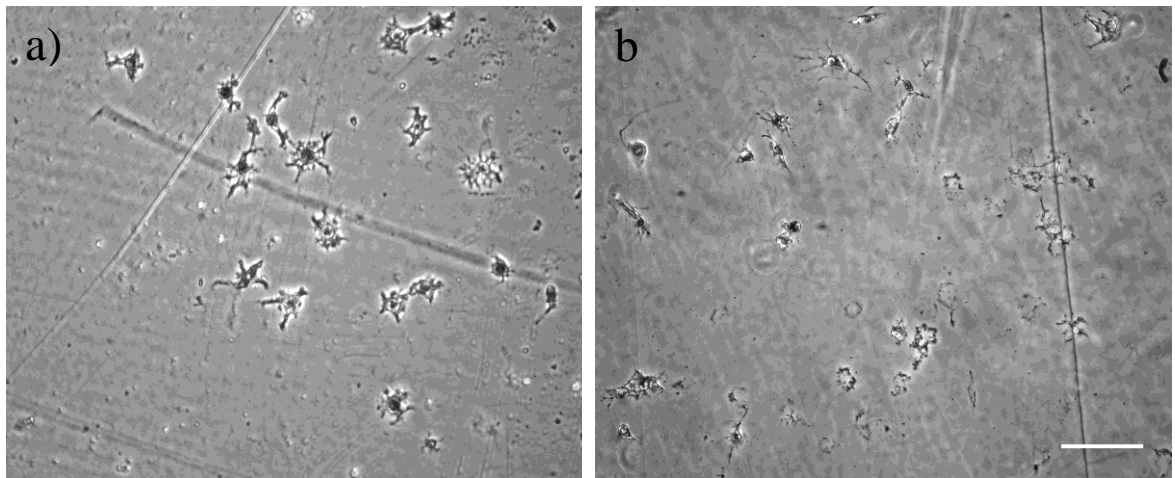
Figure 3.4: Optical microscopy images of MC3T3-E1 cell adhesion to the control substrates: (a) 1 mg/mL heat denatured BSA adsorbed to TCPS (b) 1 mg/mL heat denatured BSA adsorbed to collagen coated TCPS. The scale bar represents 100 μm.
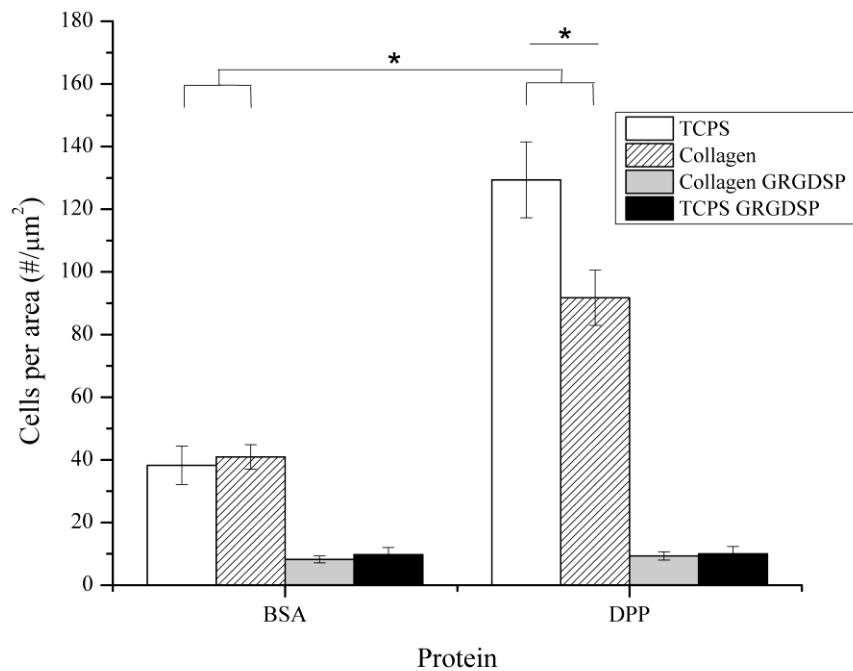
Figure 3.5: Average number of MC3T3-E1 cells (cells/mm^2) that adhered to TCPS and collagen coated TCPS with adsorbed BSA or DPP in the presence or absence of 1.0 mM GRGDSP. The adhesion data is presented as the mean ± standard error of the mean from nine samples completed over a total of three separate occasions. The inhibition data are presented as the mean ± standard error of the mean from nine samples completed over a total of three separate occasions. Three optical microscopy images were collected and analyzed for each sample completed. *Represents a statistically significant difference between the surfaces being compared (p<0.05).

CHAPTER 4. SIBLINGS AND THEIR EFFECTS ON COLLAGEN-I FIBRILLOGENESIS

4.1 Introduction

The extracellular matrix (ECM) of bone is a highly complex microenvironment containing a variety of proteins and growth factors. One of the major constituents in the ECM of newly forming bone is collagen, which provides structural support to the scaffold and a framework which allows further growth of osteogenic cells in an organized manner. While there is a general consensus regarding the overall process of collagen fibrillogenesis, there is a poor understanding of the roles noncollagenous proteins play in early collagen fibrillogenesis and the role these proteins play in helping to form the scaffold. A recent study has suggested that several noncollagenous proteins present during the stages of early bone formation can aid the fibrillogenesis process by acting as chaperones.[55] The primary group of noncollagenous proteins found in bone tissue is the SIBLING family of proteins and it has been suggested that they may assist in the early stages of collagen fibrillogenesis and scaffold development.[22,24,34,35,46,56,57]

This work seeks to explore the roles of BSP, DPP, and OPN in the early stages of collagen fibrillogenesis. Elucidating the roles that these proteins play in collagen assembly would be useful in bone biology and could aid in guiding the design of bone tissue engineering scaffolds. This study is one of the first to explore the relationships between collagen and SIBLINGs in an *in vitro* manner.

4.2 Experimental Procedures

4.2.1 Materials

Ultrapure water (18.2 MΩ-cm) was obtained from a Millipore Synergy UV water purifier (Billerica, MA) and it was used for all experiments. NaCl, Na_2HPO_4, and tris(hydroxymethyl)aminomethane (Tris-HCl) were purchased from Thermo Fisher Scientific (Waltham, MA). NaOH was purchased from Sigma-Aldrich (Saint Louis, MO). 2x fibrillogenesis buffer was made in ultrapure water with 150 mM NaCl, 30 mM Tris-HCl, and 30 mM Na_2HPO_4, after which the pH was set to 7.5 with 10 M NaOH. Collagen type I from rat tail tendon with a purity >90% was purchased from BD Biosciences (Bedford, MA).

4.2.2 Fibrillogenesis Assays

The fibrillogenesis assay was adapted from a procedure previously published by Williams et al.[12,58] The fibrillogenesis buffer, water, and well plate were preheated to 37 °C before beginning the assay. SIBLINGs were stored at 0 °C in water and the stock collagen solution was stored in a refrigerator at 4 °C. Collagen was added to the well plate along with enough protein to produce a molar ratio of 1:8, 1:16, and 1:40 (SIBLING:collagen), resulting in overall collagen concentrations of 0.05, 0.10, and 0.25 mg/mL, respectively. The amount of SIBLING used was held constant for all experiments. This was followed by adding 125 μL of 2X fibrillogenesis buffer and enough ultrapure water to give a final volume of 250 μL in each well, resulting in a final collagen concentration of 25 μg/mL. In the cases where SIBLING proteins were added, the amount of water in each well was adjusted to keep the total volume at 250 μL. All

fibrillogenesis assays were performed in a PowerWave XS2 multi-well plate reader from BioTek (Winooski, VT) and absorbance was measured at 400 nm every 3 minutes for 5 hours. The plate reader was preheated to 37 ^{o}C prior to inserting the well plate. Each column consisted of 7 available wells (n=7) and the assay was repeated 3 times for a total of 21 replicates. The data are presented as the mean of all wells in each column of the well plate.

4.3 Results and Discussion

Results from the collagen fibrillogenesis assays are shown in Figures 4.1 – 4.3. At a collagen concentration of 0.05 mg/mL, BSP and OPN reached a plateau 11% and 22% faster than the collagen control, although the final extent of fibrillogenesis was nearly identical to the collagen control. The rate of fibrillogenesis in the presence of BSP and OPN was improved by 13.3% and 14.5%, respectively, over the collagen control when 0.05 mg/mL was present in the wells. However, when the concentration was increased to 0.10 or 0.25 mg/mL of collagen, the effects of BSP and OPN with respect to rate and extent were not significantly different from the collagen control. Conversely, DPP significantly reduced both the rate and extent of the collagen fibrillogenesis at all three collagen concentrations tested, even at concentrations where the effects from BSP and OPN were washed out. It should be noted that as the concentration of collagen increases, the effects of the SIBLINGs will become more and more similar to the collagen control. This is expected because the amount of SIBLING used in the assay was held constant; the effects of SIBLING are washed out as more collagen is added to the system.

4.4 Conclusions

BSP, DPP, and OPN and their effects on early stage collagen fibrillogenesis were examined in this study. Fibrillogenesis assays revealed that both BSP and OPN improved the rate of fibrillogenesis compared to a collagen control at the lowest concentration tested. Collagen in the presence of BSP and OPN also reached a plateau slightly faster than the collagen control at the lowest concentration tested. While there was no statistically significant difference between BSP and OPN, OPN slightly outperformed BSP in terms of increasing the rate and reaching plateau. DPP significantly reduced both the rate and extent of fibrillogenesis even when the effects of the other two SIBLINGs tested were washed out at higher collagen concentrations.

Figure 4.1: Collagen fibrillogenesis assay performed with BSP, DPP, and OPN at 37 ^{o}C with 0.05 mg/mL of collagen. The data are presented as the mean ± the standard deviation of all results from each independent experiment. A * indicates $p<0.05$ for DPP with respect to collagen.

Figure 4.2: Collagen fibrillogenesis assay performed with BSP, DPP, and OPN at 37 ^{o}C with 0.10 mg/mL of collagen. The data are presented as the mean ± the standard deviation of all results from each independent experiment. A * indicates $p < 0.05$ for DPP with respect to collagen.
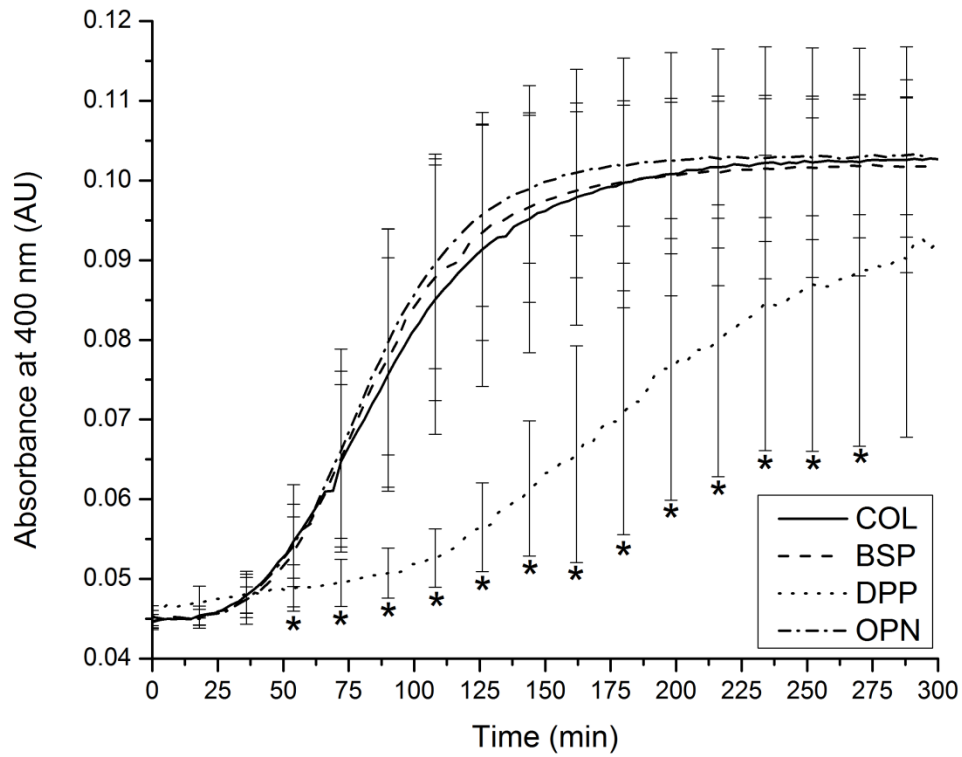
Figure 4.3: Collagen fibrillogenesis assay performed with BSP, DPP, and OPN at 37 ^{o}C with 0.25 mg/mL of collagen. The data are presented as the mean ± the standard deviation of all results from each independent experiment. A * indicates $p < 0.05$ for DPP with respect to collagen.
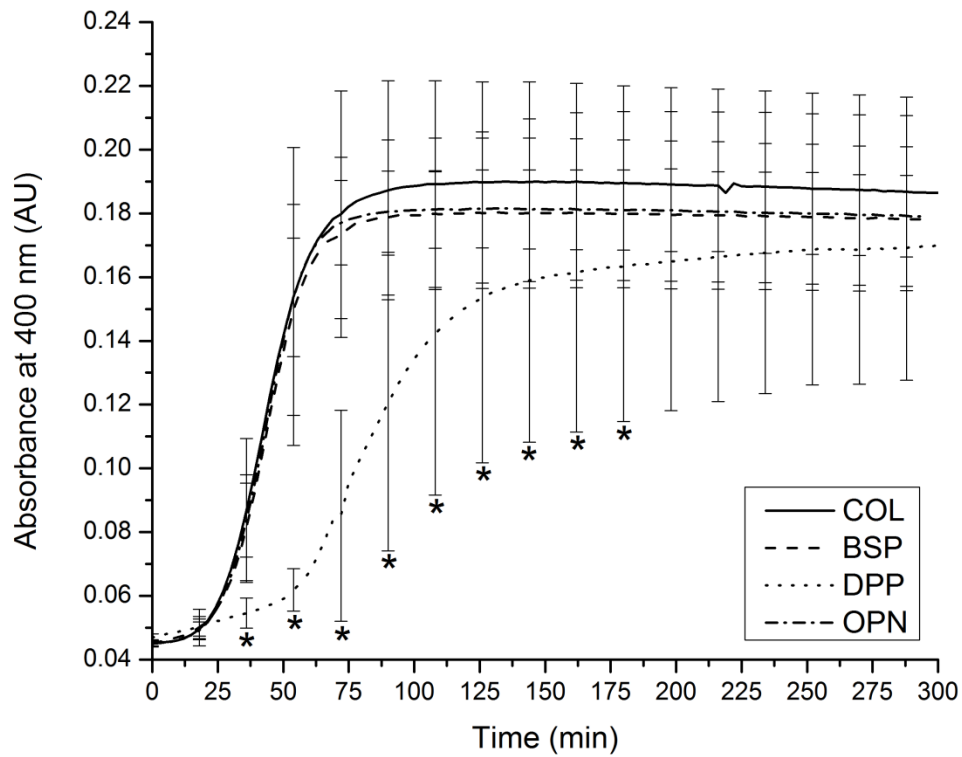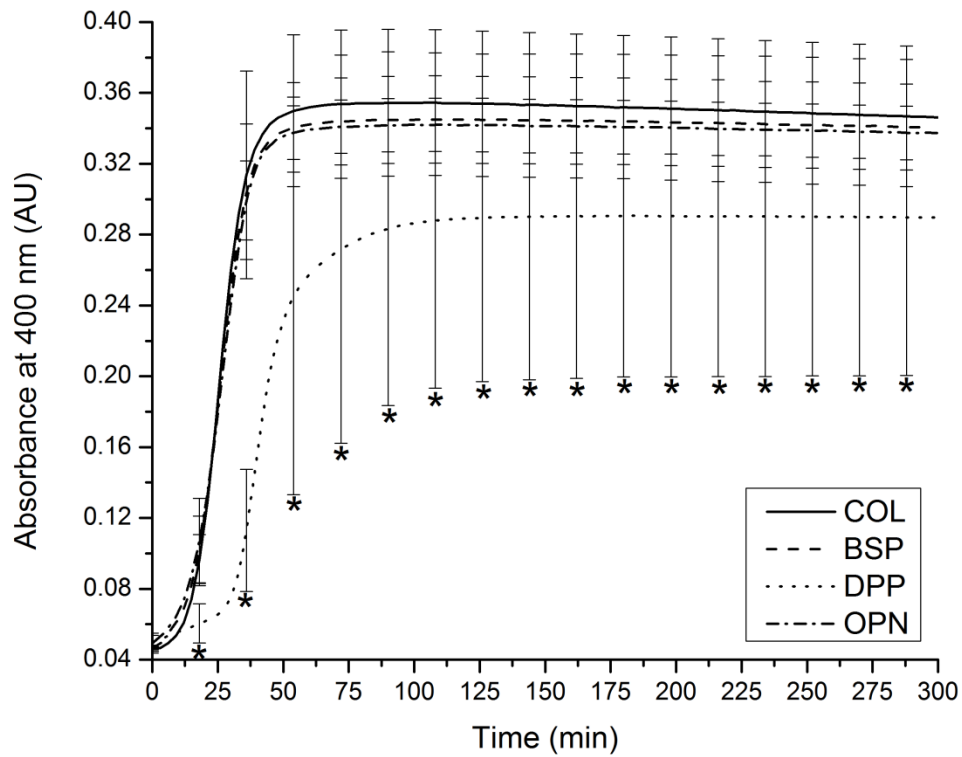
CHAPTER 5. CONCLUSIONS AND RECOMMENDED FUTURE WORK

The research presented in this work has proposed replicating the native binding interactions present in newly forming bone for use as a novel bone tissue engineering scaffold. This type of scaffold would meet the ideal characteristics of a bone tissue scaffold including biocompatibility, osseoconductivity, mechanical properties similar to that of natural bone tissue, adequate pore size and structure, and the ability to fully integrate with existing bone tissue. By mimicking the *in vivo* environment, it will reduce or eliminate unfavorable immune response, thereby minimizing or removing the need for costly and invasive secondary procedures while promoting ingrowth of the patients own bone cells into the scaffold.

It was found the DPP best simulates newly forming bone minerals in the presence of a simulated body fluid. It is unclear, however, if this would hold true in a three dimensional scaffold due to diffusion effects and other phenomena typically found in a porous scaffold. Furthermore, it was suspected that some of the mineralization effects seen in BSP and OPN were due to ion depletion from the bulk mineralization solution. Because of this, it may be of interest to explore mineralization effects in a system where the simulated body fluid is either continually refreshed or flowed across the surface of the two dimensional substrate. It would also be of interest to explore

systems with longer time intervals to determine the extent of mineral maturation that occurs in this system.

This work showed that DPP exhibited a negative orientation for cell binding when specifically bound to collagen-I, with a small increase in binding capacity when randomly adsorbed to a surface. In other work, OPN was shown to promote cell attachment to a loosely aligned collagen matrix similar to that found in newly developing bone. In particular, it was shown to have a positive orientation for cell attachment when specifically bound to collagen-I. At the same time, no significant difference in cell binding was observed between randomly oriented BSP and BSP specifically bound to collagen. Given these results, it is clear that among the SIBLINGs examined, OPN is the best protein to use to encourage cellular adhesion to a collagen matrix. It may be interesting to perform a similar set of cell attachment assays using hydroxyapatite as the substrate instead of collagen to probe the capacity of these proteins to aid cell binding to bone mineral.

In examining the roles of SIBLING proteins in collagen fibrillogenesis, it was found that among BSP, DPP, and OPN, OPN performed the best at increasing both the rate and extent of fibrillogenesis relative to the collagen control at a low collagen concentration. BSP also reached plateau sooner than the collagen control and also showed an increase in rate compared to the collagen control the low concentration. However, it should be noted that the difference between BSP and OPN was not statistically significant at any of the collagen concentrations tested. Interestingly, DPP

significantly reduced both the rate and extent of collagen fibrillogenesis, even at higher concentrations where the effects of BSP and OPN were washed out.

This work was important in providing the initial characterization of relevant SIBLINGs for later use in a bone tissue engineering scaffold. The addition of DPP to a collagen matrix was found to produce minerals consistent in morphology with those found in developing bone. After comparing cell binding in the presence of DPP-coated collagen to similar studies with BSP and OPN, OPN was found to have the best cell binding capacity when specifically bound to a collagen network. Finally, OPN and BSP were shown to increase the rate of collagen fibrillogenesis, while DPP was shown to inhibit collagen fibrillogenesis even at higher collagen concentrations where the effects from BSP and OPN were washed out. The results of this work indicate that SIBLINGs are worthy of further study as a material for constructing a biomimetic bone tissue scaffold.

References

1. Shu-Tung L. Biologic Biomaterials. The Biomedical Engineering Handbook, Second Edition. 2 Volume Set: CRC Press; 1999.

2. Steven S, Joseph C. Biomaterials. The Biomedical Engineering Handbook, Second Edition. 2 Volume Set: CRC Press; 1999.

3. Ratner BD, Bryant SJ. Biomaterials: Where we have been and where we are going. Volume 6; 2004. p 41-75.

4. LeGeros RZ. Calcium Phosphate-Based Osteoinductive Materials. Chemical Reviews 2008;108(11):4742-4753.

5. Billotte W. Ceramic Biomaterials. The Biomedical Engineering Handbook, Second Edition. 2 Volume Set: CRC Press; 1999.

6. Gokhale JA, Boskey AL, Robey PG. The Biochemistry of Bone. In: Marcus RF, D.; Kelsey, J.;, editor. Osteoporosis, Second Edition. San Diego: Academic Press; 2001. p 107 - 188.

7. Kadler KE, Holmes DF, Trotter JA, Chapman JA. Collagen fibril formation. Biochem. J. 1996;316(1):1-11.

8. Prockop DJ, Fertala A. The Collagen Fibril: The Almost Crystalline Structure. Journal of Structural Biology 1998;122(1–2):111-118.

9. Baselt DR, Revel JP, Baldeschwieler JD. Subfibrillar structure of type I collagen observed by atomic force microscopy. Biophysical Journal 1993;65(6):2644-2655.

10. Christiansen DL, Huang EK, Silver FH. Assembly of type I collagen: fusion of fibril subunits and the influence of fibril diameter on mechanical properties. Matrix Biology 2000;19(5):409-420.

11. Jiang F, Hörber H, Howard J, Müller DJ. Assembly of collagen into microribbons: effects of pH and electrolytes. Journal of Structural Biology 2004;148(3):268-278.

12. Williams BR, Gelman RA, Poppke DC, Piez KA. Collagen fibril formation. Optimal in vitro conditions and preliminary kinetic results. Journal of Biological Chemistry 1978;253(18):6578-6585.

13. Li Y, Asadi A, Monroe MR, Douglas EP. pH effects on collagen fibrillogenesis in vitro: Electrostatic interactions and phosphate binding. Materials Science and Engineering: C 2009;29(5):1643-1649.

14. Traub W, Arad T, Weiner S. Origin of Mineral Crystal Growth in Collagen Fibrils. Matrix 1992;12(4):251-255.

15. Veis A. Mineral-matrix interactions in bone and dentin. Journal of Bone and Mineral Research 1993;8(SUPPL. 2):S493-S497.

16. Hong S, Hong S, Kohn D. Nanostructural analysis of trabecular bone. Journal of Materials Science: Materials in Medicine 2009;20(7):1419-1426.

17. Boskey AL, Myers ER. Is bone mineral crystal size a significant contributor to [ldquo]bone quality[rdquo]? IBMS BoneKEy 2004;1(10):4-7.

18. Eppell SJ, Tong W, Lawrence Katz J, Kuhn L, Glimcher MJ. Shape and size of isolated bone mineralites measured using atomic force microscopy. Journal of Orthopaedic Research 2001;19(6):1027-1034.

19. Malaval L, Monfoulet L, Fabre T, Pothuaud L, Bareille R, Miraux S, Thiaudiere E, Raffard G, Franconi J-M, Lafage-Proust M-H and others. Absence of bone sialoprotein (BSP) impairs cortical defect repair in mouse long bone. Bone 2009;45(5):853-861.

20. Milan AM, Sugars RV, Embery G, Waddington RJ. Adsorption and interactions of dentine phosphoprotein with hydroxyapatite and collagen. European Journal of Oral Sciences 2006;114(3):223-231.

21. Prasad M, Butler WT, Qin C. Dentin sialophosphoprotein in biomineralization. Connective Tissue Research 2010;51(5):404-417.

22. Giachelli CM, Steitz S. Osteopontin: a versatile regulator of inflammation and biomineralization. Matrix Biology 2000;19(7):615-622.

23. George A, Veis A. Phosphorylated Proteins and Control over Apatite Nucleation, Crystal Growth, and Inhibition. Chemical Reviews 2008;108(11):4670-4693.

24. Ganss B, Kim RH, Sodek J. Bone sialoprotein. Critical Reviews in Oral Biology and Medicine 1999;10(1):79-98.

25. Sodek J, Ganss B, McKee MD. Osteopontin. Critical Reviews in Oral Biology and Medicine 2000;11(3):279-303.

26. Yamakoshi Y. Dentin sialophosphoprotein (DSPP) and dentin. Journal of Oral Biosciences 2008;50(1):33-44.

27. Baht GS, Hunter GK, Goldberg HA. Bone sialoprotein-collagen interaction promotes hydroxyapatite nucleation. Matrix Biology 2008;27(7):600-608.

28. Gordon JAR, Tye CE, Sampaio AV, Underhill TM, Hunter GK, Goldberg HA. Bone sialoprotein expression enhances osteoblast differentiation and matrix mineralization in vitro. Bone 2007;41(3):462-473.

29.   Bernards MT, Qin C, Ratner BD, Jiang S. Adhesion of MC3T3-E1 cells to bone sialoprotein and bone osteopontin specifically bound to collagen I. Journal of Biomedical Materials Research Part A 2008;86A(3):779-787.

30.   Qin C, Brunn JC, Cadena E, Ridall A, Tsujigiwa H, Nagatsuka H, Nagai N, Butler WT. The expression of dentin sialophosphoprotein gene in bone. Journal of Dental Research 2002;81(6):392-394.

31.   MacDougall M, Simmons D, Luan X, Nydegger J, Feng J, Gu TT. Dentin Phosphoprotein and Dentin Sialoprotein Are Cleavage Products Expressed from a Single Transcript Coded by a Gene on Human Chromosome 4. Journal of Biological Chemistry 1997;272(2):835-842.

32.   Wilson CJ, Clegg RE, Leavesley DI, Pearcy MJ. Mediation of biomaterial-cell interactions by adsorbed proteins: A review. Tissue Engineering 2005;11(1-2):1-18.

33.   Bernards MT, Qin C, Jiang S. MC3T3-E1 cell adhesion to hydroxyapatite with adsorbed bone sialoprotein, bone osteopontin, and bovine serum albumin. Colloids and Surfaces B: Biointerfaces 2008;64(2):236-247.

34.   Liu L, Qin C, Butler WT, Ratner BD, Jiang S. Controlling the orientation of bone osteopontin via its specific binding with collagen I to modulate osteoblast adhesion. Journal of Biomedical Materials Research Part A 2007;80A(1):102-110.

35.   Liu L, Chen S, Giachelli CM, Ratner BD, Jiang S. Controlling osteopontin orientation on surfaces to modulate endothelial cell adhesion. Journal of Biomedical Materials Research - Part A 2005;74(1):23-31.

36.   Chen S, Liu L, Zhou J, Jiang S. Controlling antibody orientation on charged self-assembled monolayers. Langmuir 2003;19(7):2859-2864.

37.   Teixeira S, Fernandes MH, Ferraz MP, Monteiro FJ. Proliferation and mineralization of bone marrow cells cultured on macroporous hydroxyapatite scaffolds functionalized with collagen type I for bone tissue regeneration. Journal of Biomedical Materials Research Part A 2010;95A(1):1-8.

38.   Jensen T, Dolatshahi-Pirouz A, Foss M, Baas J, Lovmand J, Duch M, Pedersen FS, Kassem M, Bünger C, Søballe K and others. Interaction of human mesenchymal stem cells with osteopontin coated hydroxyapatite surfaces. Colloids and Surfaces B: Biointerfaces 2010;75(1):186-193.

39.   Butler WT. Macromolecules of Extracellular Matrix: Determination of Selective Structures and Their Functional Significance. Connective Tissue Research 2008;49(6):383-390.

40.   Goldberg HA, Warner KJ, Li MC, Hunter GK. Binding of bone sialoprotein, osteopontin and synthetic polypeptides to hydroxyapatite. Connective Tissue Research 2001;42(1):25-37.

41.   Puleo DA, Nanci A. Understanding and controlling the bone-implant interface. Biomaterials 1999;20(23-24):2311-2321.

42.   Roach HI. Why does bone matrix contain non-collagenous proteins? The possible roles of osteocalcin, osteonectin, osteopontin and bone sialoprotein in bone mineralisation and resorption. Cell Biology International 1994;18(6):617-628.

43.   Prince CW, Oosawa T, Butler WT, Tomana M, Bhown AS, Bhown M, Schrohenloher RE. Isolation, characterization, and biosynthesis of a phosphorylated glycoprotein from rat bone. Journal of Biological Chemistry 1987;262(6):2900-2907.

44.   Qin C, Brunn JC, Jones J, George A, Ramachandran A, Gorski JP, Butler WT. A comparative study of sialic acid-rich proteins in rat bone and dentin. European Journal of Oral Sciences 2001;109(2):133-141.

45.   Qin C, Brunn JC, Baba O, Wygant JN, McIntyre BW, Butler WT. Dentin sialoprotein isoforms: Detection and characterization of a high molecular weight dentin sialoprotein. European Journal of Oral Sciences 2003;111(3):235-242.

46.   Huang B, Sun Y, MacIejewska I, Qin D, Peng T, McIntyre B, Wygant J, Butler WT, Qin C. Distribution of SIBLING proteins in the organic and inorganic phases of rat dentin and bone. European Journal of Oral Sciences 2008;116(2):104-112.

47.   Feng C, Keisler DH, Fritsche KL. Dietary omega-3 polyunsaturated fatty acids reduce IFN-γ receptor expression in mice. Journal of Interferon and Cytokine Research 1999;19(1):41-48.

48.   Oyane A, Onuma K, Ito A, Kim H-M, Kokubo T, Nakamura T. Formation and growth of clusters in conventional and new kinds of simulated body fluids. Journal of Biomedical Materials Research 2003;64A(2):339-348.

49.   Gungormus M, Fong H, Kim IW, Evans JS, Tamerler C, Sarikaya M. Regulation of in vitro Calcium Phosphate Mineralization by Combinatorially Selected Hydroxyapatite-Binding Peptides. Biomacromolecules 2008;9(3):966-973.

50.   Dorozhkin SV, Dorozhkina EI. The influence of bovine serum albumin on the crystallization of calcium phosphates from a revised simulated body fluid. Colloids and Surfaces A: Physicochemical and Engineering Aspects 2003;215(1-3):191-199.

51.   Lu HB, Campbell CT, Graham DJ, Ratner BD. Surface characterization of hydroxyapatite and related calcium phosphates by XPS and TOF-SIMS. Analytical Chemistry 2000;72(13):2886-2894.

52.   Omelon SJ, Grynpas MD. Relationships between Polyphosphate Chemistry, Biochemistry and Apatite Biomineralization. Chemical Reviews 2008;108(11):4694-4715.

53. Gilbert M, Giachelli CM, Stayton PS. Biomimetic peptides that engage specific integrin-dependent signaling pathways and bind to calcium phosphate surfaces. Journal of Biomedical Materials Research Part A 2003;67A(1):69-77.

54. Butler WT, Bhown M, DiMuzio MT, Cothran WC, Linde A. Multiple forms of rat dentin phosphoproteins. Archives of Biochemistry and Biophysics 1983;225(1):178-186.

55. Kadler KE, Hill A, Canty-Laird EG. Collagen fibrillogenesis: fibronectin, integrins, and minor collagens as organizers and nucleators. Current Opinion in Cell Biology 2008;20(5):495-501.

56. Butler WT, Ritchie H. The nature and functional significance of dentin extracellular matrix proteins. International Journal of Developmental Biology 1995;39(1):169-179.

57. Chen Y, Bal BS, Gorski JP. Calcium and collagen binding properties of osteopontin, bone sialoprotein, and bone acidic glycoprotein-75 from bone. Journal of Biological Chemistry 1992;267(34):24871-24878.

58. Gelman RA, Williams BR, Piez KA. Collagen fibril formation. Evidence for a multistep process. Journal of Biological Chemistry 1979;254(1):180-186.

VITA

Kevin Michael Zurick was born January 24, 1987 in Saint Louis, Missouri. He was accepted to the MU Department of Chemical Engineering as a Holtsmith Fellow in the Bernards Research Group in August 2009. He completed all necessary requirements to earn a Doctor of Philosophy degree in Chemical Engineering in December 2013. He received a B.S. degree in Chemical Engineering from Rose-Hulman Institute of Technology (2009). In addition to his research, Kevin was a Teaching Assistant for Chemical Engineering Unit Operations for seven semesters and has also worked at Procter and Gamble in Saint Louis, MO as a chemical engineering intern.